

Fluidic assembly at the microscale: progress and prospects

Nathan B. Crane · Onursal Onen · Jose Carballo ·
Qi Ni · Rasim Guldiken

Received: 11 June 2012 / Accepted: 10 September 2012 / Published online: 5 October 2012
© Springer-Verlag 2012

Abstract Assembly permits the integration of different materials and manufacturing processes to increase system functionality. It is an essential step in the fabrication of useful systems across size scales from buildings to molecules. However, at the microscale, traditional “grasp and release” assembly methods and chemically inspired self-assembly processes are less effective due to scaling effects. Many methods have been developed for improving microscale assembly. Often these methods include fluidic forces or the use a fluidic medium in order to enhance their performance. This paper reviews basic assembly theory and modeling methods. Three basic assembly strategies (tool-directed, process-directed, and part-directed) are proposed for categorizing these methods. It then summarizes progress in using fluidic forces (surface tension, viscous) and external fields (magnetic, electric, light) to aid microscale assembly. Applications of recent advances in both continuous flow and digital microfluidics in microscale assembly are also addressed.

Keywords Assembly · Microfluidics · Microscale · Self-assembly · Tool-directed · Part-directed · Capillary · Surface tension · Magnetic · Electrostatic · Acoustic · Bacteria swarm · Assembly theory · Assemblability

1 Introduction

Typically assembly processes have been the domain of manufacturing, kinematics, and mechanics. However, at

the microscale, traditional assembly techniques are not as effective for reasons described below. In the search for alternative approaches, fluid-mediated assembly methods have provided many promising methods. As these methods progress from basic demonstrations toward implementation, it becomes increasingly important for the practitioners of fluid assembly to be aware of the theory and methods for traditional assembly. Therefore, this review article provides a short introduction to the literature in assembly and assembly modeling in addition to reviewing advances in fluidic assembly.

Assembly connects physically distinct parts into a system. For most of history, assembly has been done by hand. While we have built-in visual and force feedback, dexterous manipulators, and intelligence; human ability to replicate precise motion is limited. With the advent of robots in the 1970s and 1980s, interest grew in using robots to automate assembly processes. However, engineers quickly realized that many apparently simple assembly processes were not easily performed by robots. For example, with limited degrees of freedom, careful design of fixtures was required to reliably grasp many parts (Dechev et al. 2005; Yeung and Mills 2004). Additionally, art insertion can be very sensitive to the system compliance and the assembly trajectory (Meitinger and Pfeiffer 1994, 1997; Whitney et al. 1983; Whitney 1982; Whitney and Nevins 1982). This has spurred many studies of assemblies, assembly design, and assembly processes (Boothroyd et al. 2002; Whitney 2004).

The traditional approach to assembly could be defined as “grasp and release”. Each component is located, grasped, positioned, and then released. At the macroscale, these processes are executed easily with little thought. However, each of these tasks becomes more difficult at the microscale.

N. B. Crane (✉) · O. Onen · J. Carballo · Q. Ni · R. Guldiken
Mechanical Engineering Department, University of South
Florida, 4200 E. Fowler Ave ENB 118, Tampa, FL 33620, USA
e-mail: ncrane@usf.edu

When people assemble macroscale objects, part location is a simple visual task. As part size decreases, visual location of parts becomes more challenging due to the limited depth of focus and resolution of optical observations. Assembly has been done inside an SEM (Kasaya et al. 1999) and using novel optical imaging systems (Potsaid et al. 2005, 2006) to address this challenge. Additionally, grippers can block views of the parts (Enikov and Lazarov 2001).

One solution is to use sensorless systems that can reliably orient and locate a part so that it can be grasped for assembly (Erdmann and Mason 1988; Liu et al. 2011a). These techniques use a series of forces or system changes that can either orient and locate a single part or filter out all mis-oriented components with minimal information about its initial position and orientation. These methods include vibratory, mechanical, gravity, and pneumatic feeders (Boothroyd 2005; Goemans et al. 2006). Similarly, robots can also be designed to locate themselves with limited number of sensors (O’Kane and LaValle 2005). These results are not directly applicable to the microscale due to scaling effects and manufacturing limits (Moll et al. 2002), but they are similar in some respects to self-assembly (SA) processes. Both systems decrease the location uncertainty of the parts without direct manipulation.

At the macroscale, parts are typically grasped by friction due to compressive grasping forces. However, small parts can also be grasped using vacuum (Chen et al. 2010b), freezing (Lopez-Walle et al. 2008), and capillary forces (Vasudev et al. 2009). Force sensing and grasp compliance have been investigated for their potential to reduce part damage from rigid grasping techniques (Kim et al. 2004; Zubir et al. 2009). The grasping process itself may also be used to improve the location of the parts relative to the grippers (Ellekilde and Petersen 2006).

Once the parts are grasped, they must be moved to the desired position. Microscale manipulators often have very limited range—perhaps just a few part diameters—while the grippers and actuators are much larger than the parts. Often, microscale systems require more expensive equipment to move less valuable parts slower than their millimeter- to centimeter-scale counterparts (Das et al. 2007; Dechev et al. 2006; Dechev and Cleghorn 2002). The relatively large size of the manipulators and the limits of 2D micro-manufacturing methods complicate the simultaneous use of multiple manipulators.

However, at the microscale, the biggest challenge of “grasp and release” assembly may be the release. At microscale dimensions, the gravitational forces are often too small to reliably overcome other forces including capillary, and Van der Waals forces (Fearing 1995). Work has been done to overcome these effects using air pressure (Chen et al. 2010b), vibrations (Chen et al. 2009, 2010a),

impact (Chen et al. 2009), and the exploitation of directional variation of the forces (Feddemma et al. 2001; Kasaya et al. 1999); but this still remains a challenging problem in practice. Additional discussion of microscale “grasp and release” assembly is found in Cecil et al. (2005).

If we look at manmade systems across the size scales, microscale systems are the only area where we regularly attempt to fabricate devices without assembly. Macroscale assembly is readily done by people with increasing support from robots. Many nanoscale assemblies are still quite challenging as well, but chemical synthesis is a highly developed area of nanoscale assembly. Biological growth consists of nanoscale assembly of molecules to form cells, tissues, and entire organisms. Despite the many challenges, reliable assembly of microscale components is critical to achieve high-performance micro- and nanoscale systems.

System performance depends on both material and geometry. Both are limited without the ability to assemble. Without assembly, devices must be made in situ through a series of compatible processes and materials. This imposes significant limitations on the types of materials that can be integrated. Photolithographic fabrication often requires the successive deposition and patterning of many separate layers. Additionally, the predominately 2D nature of most microfabrication processes imposes additional design constraints. Creativity has permitted the fabrication of some remarkable devices without requiring assembly. Moreover, manufacturing and folding methods have overcome some of the limits of 2D manufacturing (Arora et al. 2006; Leong et al. 2007, 2010; Nichol et al. 2007). However, current micro-assembly systems still impose limitations on product design and performance.

Morris et al. (2005) considered the changing rates of assembly processes with size of the objects being assembled as illustrated in Fig. 1. Large objects are assembled relatively slowly—probably due to their large inertia and the customized nature of most large-scale assembly. However, as parts decrease in size, their assembly rate increases tremendously until they reach a peak at the millimeter-size scale. Below this size, assembly becomes progressively slower using traditional, directed approaches. It is clear that alternative methods are needed. Challenges arise from the physics of the microscale world that make it difficult to scale macro-assembly techniques to micro-sized components (Bang et al. 2005; Bos et al. 2008; Menciassi et al. 2004).

Significant efforts have been undertaken to develop new assembly methods that can circumvent some or all of the challenges of “grasp and release” assembly. These include alternative part-grasping techniques and processes that eliminate the need to locate individual parts, such as sensorless assembly and SA. Assembly methods that rely on fluidic forces and fluidic mediums show particular promise at the microscale.

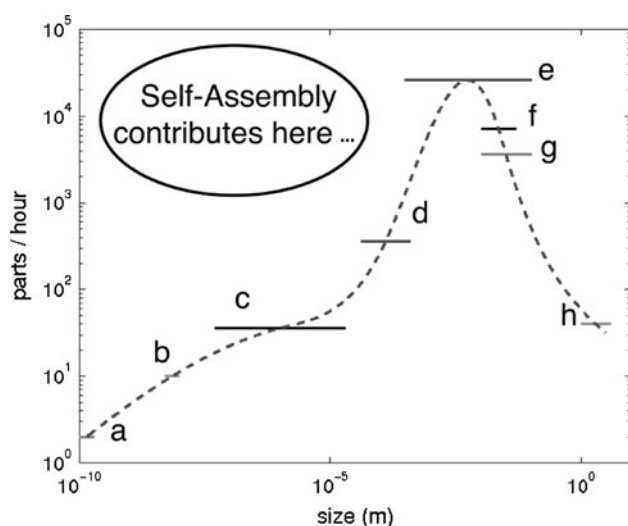


Fig. 1 Variation in assembly rates with part size. Declining rates for submillimeter parts suggest the need for alternative processes such as self-assembly (SA). Figure reproduced with permission from IEEE (Morris et al. 2005)

This review article focuses on assembly processes that use fluidic forces or require a fluidic medium. The first section reviews the motivation and challenges of microscale assembly in more detail and then summarizes key information on assembly theory that remains relevant to microscale assembly processes. The remainder of the article reviews progress in developing fluidic assembly systems for devices and features at the microscale. Microscale is defined roughly as having dimensions between 100 nm and 5 mm. It is in this general range where fluidic forces have been most widely used. One of the key methods of fluidic assembly at the microscale is self-assembly (SA). However, several excellent review articles have been published on this subject in recent years (Boncheva et al. 2003; Elwenspoek et al. 2010; Mastrangelo et al. 2009; Morris et al. 2005; Syms et al. 2003; Whitesides and Grzybowski 2002; Xia et al. 2000). In this review, we will confine ourselves to a discussion of how SA fits into the range of possible assembly methods, and focus the article on methods for directed assembly at the microscale.

2 Assembly strategies

Assembly methods can be divided into three main strategies as summarized in Table 1. These strategies are independent of the assembly size scale. Each has their particular advantages and disadvantages that are worth noting. To address these compromises, hybrids of these basic categories have also been developed. These basic strategies are discussed below.

2.1 Tool-directed assembly

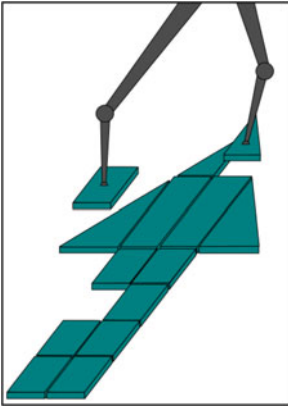
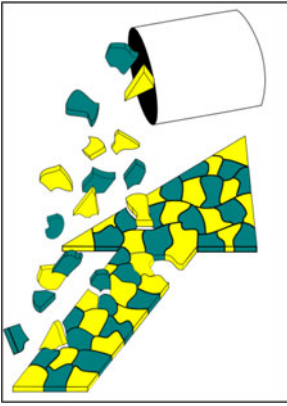
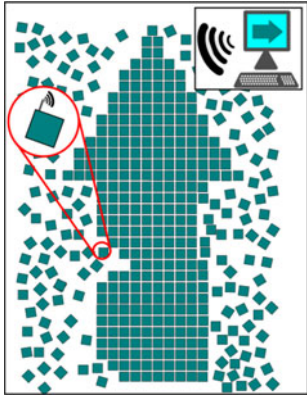
Tool-directed assembly is the traditional approach in which control over the assembly is primarily external to the parts. External agents such as people, robots, or programmable tools decide what is assembled from the parts and how it is accomplished. This is the dominant method of assembly at the macro- and mesoscale. Since the controls are external to the parts, the parts are simplified and the parts are readily reused to make different parts and assemblies. If programmable tools are used, then adjustments to the assembly output can be made quickly. The assembly outcomes are relatively insensitive to the environmental conditions at the time of assembly. Common design-for-assembly strategies would try to (1) reduce the number of parts and (2) redesign the parts to reduce the number of ways that the parts can be mis-assembled (Boothroyd et al. 2002). Due to the cost and complexity of the tools, assemblies are often done predominantly in series (i.e., assembly line).

2.2 Process-directed assembly

In process-directed assembly, the assembly outcome depends on the parts and the conditions under which they are brought together. This is the dominant assembly method at the nanoscale and it is common in chemistry. In these processes, the outcomes depend on environmental variables such as temperature and pressure as well as the reactants and their concentrations. It is often characterized by multiple assembly products. These assembly processes are massively parallel and relatively simple to execute. However, sometimes the various products must be separated (purified) to eliminate the undesired assemblies (products). The challenge of process-directed assembly is in identifying the conditions under which desirable assemblies can be created. In chemistry, centuries of experiments and theory have been devoted to understanding the conditions under which a relatively small number of building blocks can be assembled into desired products.

When this approach is applied to manmade objects, it is often called self-assembly. While chemistry is limited to the reactions of a finite set of elemental building blocks, self-assembly building blocks are infinite in number. While this offers new flexibility and possibilities, it also creates enormous challenges in designing the parts and the process to produce the desired assemblies. Due to the interest in and particular challenges of self-assembly at the microscale, it is discussed separately below. Design-for-assembly strategies modify the parts or assembly conditions to reduce assembly errors and/or increase assembly speed. The part design is heavily impacted by the nature of the assembly process.

Table 1 Summary of three key assembly strategies

	Tool-directed assembly	Process-directed assembly (self-assembly)	Part-directed assembly
Illustration			
Assembly control	Embedded in tooling Tooling can be reprogrammed Deterministic	Embedded in part/process design Limited flexibility Stochastic	Computation occurs in parts Extreme flexibility Deterministic
Parts	May be used in multiple assemblies Optimized for use performance	Assembly specific May be constrained by requirements of the assembly process	Actuation, computation, and sensing embedded in every element Reusable for multiple assemblies
Product design	Some coupling with tool design	Tightly coupled with process design	Only need to specify desired outcome
Product performance	Minimal constraints from the assembly process	Likely limited by assembly process constraints	Compromised for flexibility in assembly

2.3 Part-directed assembly

If intelligence and control can be built into the parts themselves, the parts could assemble themselves. Such a system would not need a complicated machine in order to complete the assembly. Nor would the assembly outcome have to be determined a priori as in process-directed assembly. The parts could assemble in response to external messages, pre-programmed missions, or in response to environmental stimuli. This is the essential concept of swarm robots, particularly those that can link together to accomplish specific tasks. The basic concepts of modular, reconfigurable, cooperative, and self-replicating robots have been demonstrated (Gro et al. 2006; Gross and Dorigo 2008; Klavins et al. 2006; Wei et al. 2011), but full implementation requires additional theory and technology (Yim et al. 2007).

In order to realize this approach, actuators, sensors, and computational capability all need to be embedded in the parts. This strategy is particularly effective for applications in which reconfiguration is required. Otherwise, there is significant performance and cost penalty to incorporate all of the required actuation functions, communications and computations into each individual component. Thus, this approach may only be implemented in specialized

applications. At the microscale, cells are prototypical smart parts that can respond to the environment and cooperatively accomplish tasks. Future advances may permit similar functionality to be achieved using manmade systems.

3 Assembly theory background

Automated assembly systems have been studied since the earliest days of robotics. However, as researchers attempted to apply the early robots to assembly tasks, they quickly discovered many complexities in the assembly tasks that made automation difficult. After more than 30 years, a substantial body of literature is now available that addresses many issues relevant to microscale assembly. However, many researchers working on microscale fluidic assembly may be unaware of this body of knowledge from traditional manufacturing practice. As the complexity of the assemblies increases, these theoretical underpinnings become increasingly important. Therefore, key concepts, findings, and techniques from this body of literature are summarized below, as many are applicable to all scales and methods of assembly.

3.1 Assembly modeling methods

Assembly is the joining of physically separate components to perform desired functions. Initially, each part has six independent degrees of freedom. As the parts are joined together, the spatial degrees of freedom are reduced by the connections between components. Typically, the spatial relationship between the parts is important to the function that they perform. For example, holes must align in order to insert a bolt, optical components must have a common axis, and electrical connections must line up with the correct wires. While the spatial relationships receive the greatest focus in assembly processes, other properties such as thermal and electrical resistivity of connections can also be critical.

The design of the system to be assembled and the process that assembles it are closely linked (Sprumont and Muller 1997). In fact, several authors have focused on assembly as the focal point for integrated product development processes (Boothroyd et al. 2002; Whitney 2004). Integrated product development processes simultaneously consider all aspects of the design and production to shorten design time and generate higher performance designs. This requires the use of a variety of assembly models with varying levels of fidelity for different design stages.

Modern solid modeling software permits accurate representation of component geometry and the connections between the components. This software commonly includes the ability to check for interferences and can evaluate issues of maintenance and assemblability (Boyse 1979; Jayaram et al. 2004; Seth et al. 2010). However, an accurate solid model requires detailed component

knowledge that is not available in early design steps when many of the important configuration choices are made. Thus, there is great value in alternative methods for representing assemblies that capture key aspects of the assembly performance without requiring as much detail. The simplest model of a mechanical assembly is a network diagram in which the parts are nodes and the nodes representing touching parts are connected by lines as illustrated in Fig. 2 (Whitney 2004). These simple diagrams can be helpful in comparing different schemes for accomplishing the assembly function, and identifying the parts that play a role in delivering important spatial relationships in the assembly.

While the network diagrams are easily constructed, they contain relatively limited information. Datum flow chains augment these models with directional arrows on the connecting lines to represent the path of the constraints as illustrated in Fig. 3. Each arrow is labeled with the degrees of freedom that are constrained by the connection between the two parts. Double lines are used to represent key relationships between parts that affect the assembly function. Datum flow chains provide a concise way of representing the transmission of spatial relationships between parts and can be very helpful in exploring different assembly configurations during the early stages of design and in diagnosing the causes of assembly problems (Mantripragada and Whitney 1998).

Datum flow chains reveal two basic assembly strategies (Mantripragada and Whitney 1998). In most assemblies, the part positions are completely constrained by features on the mating parts. However, in some assemblies, the parts are placed in a fixture to position them for assembly. With proper design, the fixture achieves assemblies with smaller variation than the parts. The datum flow chains can be combined with tolerance information and coordinate

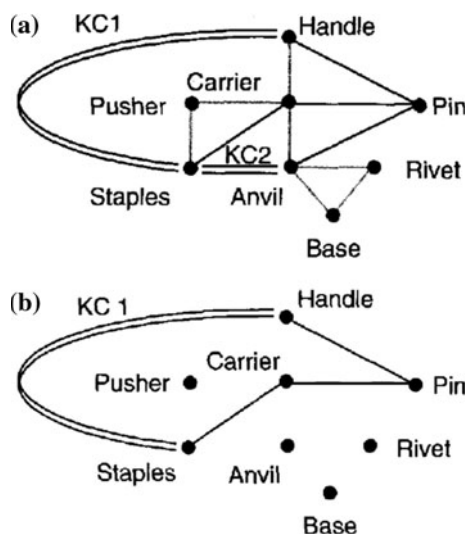


Fig. 2 **a** Liaison diagrams of a stapler represent the connections between the components. Lines show connections between parts. Double lines identify a key characteristic (KC) that affect system function. **b** Simplified liaison diagram that shows the connections that deliver one of the KCs (Whitney 2004). By permission of Oxford University Press, Inc

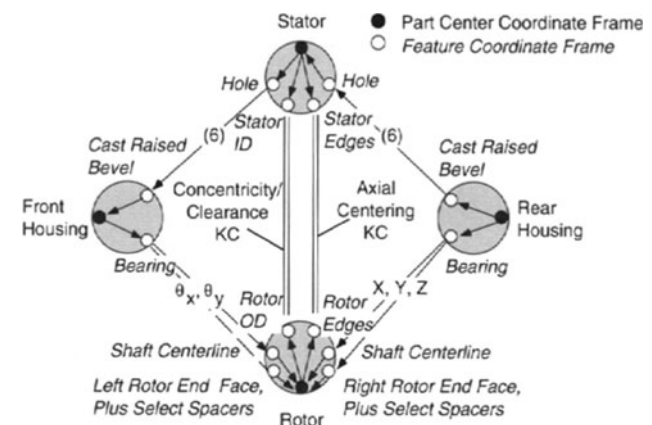


Fig. 3 Datum flow chain of an electric motor. Arrows show how constraint in different degrees of freedom is passed through different components and features within the components. Used with permission from (Whitney 2004)

transformations to predict the effect of manufacturing variation on the spatial relationships in the assembly (Chase and Greenwood 1987; Gao et al. 1998; Whitney et al. 1994).

Two of the biggest sources of assembly problems are under- and over-constraint. When parts are under-constrained, one or more degrees of freedom are free and desired spatial relationships cannot be maintained. In contrast, over-constrained assemblies have multiple features trying to locate the same degree of freedom. This results in conflicts between the features. Assembly then requires highly precise components, large clearances, and/or deformation of one or more parts in the assembly. Over-constraint errors cause sensitivity to assembly sequence, the use of large force for assembly, and unexplained part failures (Whitney 2004).

Awareness of these issues and heuristics such as the 3-2-1 location principle are sufficient to eliminate constraint problems in many assemblies (Whitney 2004). However, to design complex assemblies or automate the process for simpler assemblies, screw theory provides a more rigorous method to assess the system constraint level (Adams and Whitney 1999; Shukla and Whitney 2001, 2005). Screw theory provides an elegant mathematical framework for describing the transfer of forces and motions through a mechanical system (Davies 2006, 1983a, b, c). Using screw theory, complex assemblies can be readily analyzed for under- and over-constraint (Whitney 2004).

Application of these methods to practical connections requires some idealizations of the contact type. Often, connections are open to multiple interpretations. Whitney (2004) has prepared a library of twist matrices for common connection types. While microscale assembly uses many similar connection types, there may also be new connection types and new characteristics to be considered such as larger relative tolerances that merit additional consideration. In particular, some microscale bonding methods, such as by surface tension, may not be well-approximated as rigid connections. At the macroscale, elastic averaging is sometimes used to reduce random errors by averaging a number of elastic bonds (Awtar and Sevincer 2006; Culpepper et al. 2004; Slocum and Weber 2003). Such principles may also be applicable to many microscale fluidic assemblies.

3.2 Gross and fine assembly motions

The process of assembly is commonly broken into two steps (Whitney 2004). In the first, “gross positioning”, the part is positioned in the vicinity of the assembly position. This can be done easily with open-loop controls. The required distances and tolerances are large relative to the part dimensions. In the second step, “fine positioning”, the parts are brought into their final assembled positions. This second step imposes stringent alignment and accuracy

demands on open-loop positioning systems. For example, inserting a pin in a hole frequently requires angular alignment within a fraction of a degree and positioning within a small fraction of the pin diameter. Visual and force feedback have both been used to improve the assembly process. However, visual feedback is complicated by the limited line of sight during final assembly. Force feedback is also difficult because there is no unique mapping between the forces and the assembly condition (Whitney 1987). Substantial progress has been made in overcoming these challenges to feedback-based positioning systems (Conant-Pablos et al. 2003; Du et al. 2008).

Other techniques used in place of or to complement feedback-based systems include increased clearances, generous chamfers, and specialized gripping. Underlying these methods is a body of literature on the force–position relationships during common assembly tasks (Whitney 2004). These methods can be used to identify a range of conditions under which problems such as jamming and wedging can be avoided. One particularly effective approach is to adjust the gripping method to improve the force-insertion characteristics. A remote centered compliance (Bang et al. 2005; Whitney 1982) creates an effective center of rotation near the tip of the part being inserted. Under these conditions, the normal forces of the hole on the part act to improve the alignment so that insertion can be accomplished without force or visual feedback. It may be possible to develop analogous methods for fluidic assembly processes that improve alignment such as the semi DUO-SPASS method which uses a mechanical aperture to provide initial alignment with surface tension acting to increase the accuracy (Fang and Bohringer 2006a).

At the microscale, the forces are different as are many of the relative tolerances. However, analogous techniques could be applied to improve the ability of parts to assemble. For example, Cappelleri et al. (2011) considered strategies under which mesoscale parts could be assembled successfully by pushing them. Popa et al. (2007) addressed these problems by integrating compliance into the parts that dramatically reduce the positioning accuracies required for assembly as seen in Fig. 4.

3.3 Design of assemblies

Assembly design has many facets. At its most basic level, liaison diagrams and datum flow chains can be used to evaluate alternative ways of positioning components to achieve the required relationships in the assembled system. These high-level models support top-down assembly design in which high-level assembly requirements are identified and the constraint relationships are then used to define the lower level requirements for individual subassemblies, parts, and features on the parts.

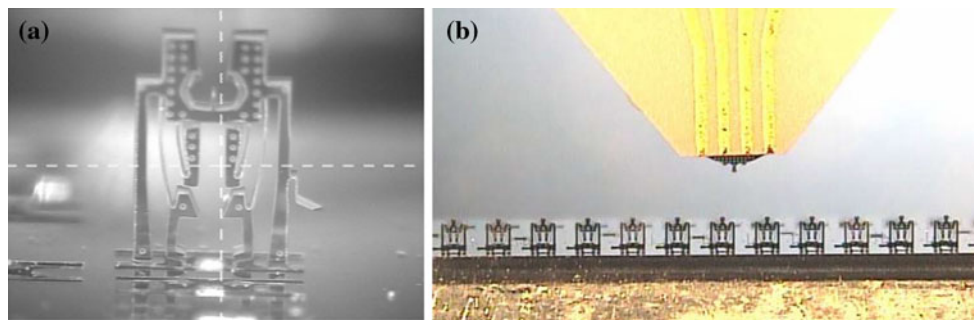
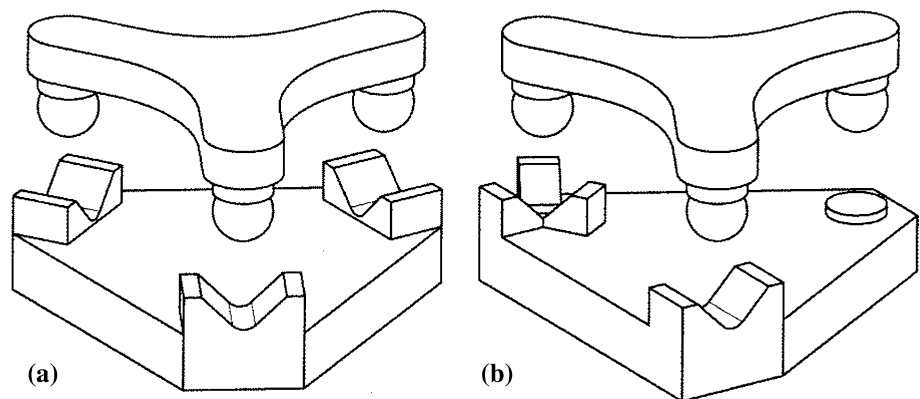


Fig. 4 Part compliance can simplify alignment requirements for assembly. **a** Compliant microparts inserted into mating holes. **b** Series of assembled parts with the assembly tool used to insert them. Parts in both figures are $800\ \mu\text{m} \times 1300\ \mu\text{m} \times 100\ \mu\text{m}$ (Das et al. 2007)

Fig. 5 Illustration of kinematic couplings for repeatable location of components. **a** Three grooves each locate two independent degrees of freedom. **b** 3-2-1 principle is applied to the kinematic coupling. From left to right, the first mate constrains three degrees of freedom, the second constrains two, and the third, one degree of freedom (Hale and Slocum 2001)



One area of assembly design that has received particular attention is the selection of features that can accurately and repeatedly locate the parts. The ideal constraint type is termed “exact” or “kinematic” constraint (Furse 1981; Hale and Slocum 2001; Schouten et al. 1997; Slocum 1988; Slocum and Donmez 1988). Lord Kelvin and J.C. Maxwell identified the unique benefits of this constraint approach in the late 1800s. (Slocum 1992) In this method, each individual positioning feature removes independent degrees of freedom. These features are often formed from special grooves that mate with spheres as illustrated in Fig. 5. Another approach to high accuracy positioning from lower accuracy components is to use elastic averaging. Elastic averaging uses multiple flexible features that elastically deform during mating (Awtar and Sevincer 2006; Marentis et al. 2009). The assembled position is the one with the minimum energy. If a large number of mating pieces with random errors come together, the assembled position reaches a repeatable mean with less error than that of the individual mating components. In many practical constraints separate features are used to determine the part position (groove/sphere pair) and to hold it there (glue, bolt).

Due to the impacts of assembly processes on the design, performance, and cost of the final system, significant efforts have been made to develop methods for assessing the assemblability of parts and components at early stages

of the design process. For example, Sony utilized a method that emphasized the drawing of exploded views of assemblies at the earliest stages of design to force engineers to consider assembly (Whitney 2004). Hitachi developed a more formal assembly design system termed Extended Assembly Evaluation Method (AEM) in which comparative methods are used to develop a relative assemblability score that can provide a standard of comparison between designs (Ohasi et al. 2002). Boothroyd et al. (2002) developed a system based on empirical data that predicts assembly times based on simple part features such as size, symmetry, and tools required. They further identified other assembly criteria including assembly efficiency and guidelines for reducing the number of parts in an assembly. Different assembly techniques favor different designs (Boothroyd and Dewhurst 1990).

An important part of the assembly process is the assembly sequence. In many cases, there are many feasible sequences while in others there may not be any. Many methods have been developed for identifying and representing feasible sequences (Fazio 1987; Gu and Liu 2008; Lanham and Dialami 2001). Important considerations include the assembly directions, reorientation requirements, and the stability of the parts that are inserted. Assembly sequence also affect production metrics such as the assembly cycle time, equipment required, cost of fixing

errors, and the lead time required to customize a product. Thus, there is a great interest in integrating many of the different assembly design issues into a single optimization system (Fazio 1987; Lanham and Dialami 2001; Sprumont and Muller 1997; Udeshi and Tsui 2005). The planar nature of microscale fabrication may simplify the identification and selection of sequence for microscale assemblies. However, the ability to control assembly sequence is still vitally important. This is currently an obstacle to the fabrication of complex assemblies via SA.

3.4 Macro-assembly and micro-assembly

Some of the macro-assembly techniques are directly applicable to microscale assemblies. For example, liaison diagrams and datum flow chains can be used to compare microscale system designs. Screw theory could be used to assess the constraint status of micro-assemblies and matrix transforms used to study the impact of tolerances on the assembly accuracy. However, in many areas, adaptations and/or extensions are required to increase the usefulness of these techniques. For example, how can kinematic constraint and/or elastic averaging be applied given the manufacturing constraints of photolithography techniques? How can fluidic bonds be used for kinematic constraint? How does design for assembly apply to novel assembly techniques such as the ones described below?

Microscale assemblies produced to date have focused on the fabrication of relatively simple systems that demonstrate individual assembly concepts. As microscale assembly systems mature, methods for modeling assemblies, designing assembly processes, and designing parts for assembly will become increasingly important.

4 Self-assembly

Self-assembly (SA) is an assembly method in which the parts are designed to assemble spontaneously when they are brought together—typically by random interactions such as by stirring or vibrating the components. SA has more in common with chemical reactions than traditional “grasp and release” assembly. Thus, SA eliminates many challenges of “grasp and release” as the parts are never grasped. The resulting equipment could be much cheaper as many assemblies can be produced in parallel to increase the process speed. The early SA work of Yeh and Smith (1994a) with fluidic self-assembly sparked significant interest in SA of microscale components. SA processes have been demonstrated with high rates and >98 % accuracy (Knuesel and Jacobs 2010; Zheng et al. 2004) and 3D capabilities (Breen 1999; Oliver et al. 2001). However, SA requires a process-directed strategy that links the assembly

process and part/system design in new ways. As SA relies on stochastic interactions to assemble the components, new types of stochastic assembly errors are introduced that require different design strategies. Fluids are often used in SA in order to provide a medium for the assembly. The fluid reduces friction and can be used to circulate the components until they contact. Additionally, fluids can provide the bonding force either through pressure (Tolley et al. 2008) or capillary affects (Syms et al. 2003). When the carrier fluids evaporate, the adhesion forces can bond components together (Yeh and Smith 1994b).

Perhaps, the biggest challenge of SA is the design of parts and processes that can achieve the desired outcome. The parts must be designed to have an energy minimum in their assembled condition. Many different types of forces have been used including capillary, electrostatic, magnetic, viscous, and chemical bonds (Pelesko 2007). Bond models have been developed for many bond types (Bohringer et al. 2001; Harsh and Lee 1998; Shetye et al. 2007; Xiong et al. 2004) that can be used to design parts for SA. However, if multiple types of parts must be assembled, it is a much greater challenge to design parts that will bond without errors (Pelesko 2007). This can be addressed through the use of different bonding types (Wu et al. 1999), integrated controls (Krishnan et al. 2008), and multi-batch assembly (Crane et al. 2009; Xiong et al. 2001). However, most of these techniques only permit the assembly of a small number of part types. Significant work is necessary in order to extend these methods to the assembly of more complex systems. Due to these challenges, most current SA systems are relatively simple structures consisting of a large number of identical parts assembled to one substrate (Jacobs et al. 2002; Knuesel and Jacobs 2010; Shetye et al. 2009) or in a repeating structure (Gracias et al. 2000). Electrically conductive bonds have been demonstrated with low melting point solders and through capillary-driven bonds between metallic plates, followed by subsequent annealing (Arscott et al. 2010; Cannon et al. 2005; Gracias et al. 2000; Zheng et al. 2004). Additional work is needed in creating more types of functional bonds with improved performance.

While laboratory demonstrations of SA for simple structures are promising, there is relatively little progress in industrial implementation at the microscale. One key challenge is the lack of process-level modeling to guide scaling from laboratory to factory. Current process models are based on experimentally measured quantities that do not provide insight into simple changes such as the size of the container, the velocity of the fluid, or the patterns of stirring (Hosokawa et al. 1994; Napp et al. 2006; Zheng et al. 2004). Better understanding of such key parameters is needed to guide the scaling of self-assembly processes to production scale.

SA faces an additional scaling problem at the microscale. This is illustrated by looking at basic assembly relationships. A basic expression for the assembly rate (\dot{a}) is

$$\dot{a} \propto nfp_a \quad (1)$$

where n is the number of parts, f frequency of assembly attempts per part and p_a is the probability of assembly per attempt. Consider the case of a cubic part of length l and density ρ assembled by capillary forces with surface tension γ . For successful bonding, the part bonding energy ($E_b \propto \gamma l^2$) must be larger than its agitation energy ($E_A \propto \rho l^3 v^2$) where ' v ' is the part velocity. If the ratio of bonding to agitation energy remains constant with scaling, then the velocity for a given bonding ratio decreases with $l^{-1/2}$. If the average distance between parts (d) scales with the part size, then the distance that the parts travel to contact the substrate increases with part size. The attempt frequency—expressed as the average velocity divided by the average distance—is then decreasing with $l^{-3/2}$. As a result, the attempt frequency of a 1 nm part is 10^6 times that of a 10 μm component.

Additional scaling factors could further reduce the assembly rate. Thus, SA processes that work well at the molecular levels become much slower at larger size scales. Successful assembly must focus on achieving a high assembly probability and/or very high levels of parallel assembly. Many SA processes increase the assembly probability by reducing the spatial degrees of freedom either by assembling from a liquid interface (Bowden et al. 2001; Knuesel and Jacobs 2010; Whitesides and Grzybowski 2002; Wolfe et al. 2003) or by folding the parts from an initial configuration (Arora et al. 2007; Harsh and Lee 1998; Leong et al. 2007). Mechanical techniques to improve alignment before final assembly offer another alternative (Fang and Bohringer 2006b).

5 Position/actuation via capillary forces

Capillary forces deserve considerable emphasis within the topic of microscale assembly. They are large relative to gravitational forces at the microscale. Hence, they must be taken into consideration when designing any microscale assembly mechanism. This section provides a brief theoretical background on capillarity, as well as a review of efforts that utilize capillary interactions as a mechanism for assembly.

Capillary force exists at the interface of two or more immiscible fluids. All surfaces possess a certain free energy different from their bulk characteristics. It is especially apparent for liquids because they readily deform to minimize the free energy. This free energy (J/m^2) is often referred to as surface tension (N/m). This creates a pressure difference (ΔP) across a liquid interface given the Laplace equation $\Delta P = \gamma(1/R_1 + 1/R_2)$ where R_1 and R_2 are the

principle radii of curvature of the surface. The pressure difference is called the Laplace pressure. As the drop's size decreases, the Laplace pressure increases. At the macro-scale, capillary forces are small compared to gravitational force. As the length scale of assembly decreases, capillary force becomes more dominant. At the microscale, force magnitudes are adequate enough for manipulating components. At nanoscale, however, capillary forces can be strong enough to cause unwanted deformations. The large free energy of small droplets also makes it difficult to form sub-micron fluid patterns. Thus, capillary forces are primarily used for microscale applications.

For many assembly applications, it is essential to modulate the capillary forces, spatially and/or temporarily. Surface tension can be readily manipulated by a variety of methods. Below are some commonly used methods and their operating principles:

- **Thermal** Surface tension is sensitive to temperature changes. For most liquids, surface tension decreases when temperature increases. When there is a temperature gradient present (either due to local heat transfer or evaporation), surface tension gradient causes the liquid to flow from the area of lower surface tension to that of higher surface tension (Lappa 2010). "Thermocapillary convection" or Marangoni effect can be used to manipulate floating or suspended parts (Adachi et al. 1995; Hu and Larson 2006; Di Leonardo et al. 2009).
- **Surfactants** Many materials and even solid particles segregate to interfaces where they lower the interfacial energy. Organic surfactants (or surface active materials) usually consist of two ends: one lyophobic and one lyophilic end. Once in a solution, surfactant molecules migrate to and align on the surface with the lyophobic ends facing away from the solvent. This phenomenon change the surface energy of the liquid (de Gennes et al. 2004; Myers 1991). Surfactants prevent coalescence in droplet-based microfluidics and control protein adsorption on liquid–liquid interfaces (Baret et al. 2009; Roach et al. 2004). Surfactants are very effective but the surface energy changes are not easily reversible.
- **Coatings** Spatial modulation of capillary forces is readily obtained by applying different coatings to the surfaces. One useful approach is to pattern self-assembled monolayers (SAM) on a substrate via soft lithography (Kumar and Whitesides 1993; Rogers and Nuzzo 2005). Both hydrophobic and hydrophilic surfaces can be created by selecting an appropriate SAM. A wide variety of SAM molecules are commercially available for many common surfaces. It is also possible to apply coatings that change their wetting properties in response to environmental conditions such as pH and temperature (Dong et al. 2006; Vidyasagar et al. 2008).

Although the monolayer thickness of a SAM may be convenient for many applications, these coatings can be delicate, and environmentally sensitive. Therefore, in many cases, thicker coatings are more favorable. Metals, organic- and fluoro-polymer coatings can also change the surface energy. Deposition processes such as spin coating, dip coating, PVD and CVD are quite standard (Kim et al. 2006; Xu et al. 2012).

- **Surface roughness** Microfabrication techniques such as DRIE (deep reactive ion etching), laser etching and polymer micro-molding enable the control of surface roughness by creating micro/nanoscale structure (Cansoy et al. 2011; Ding et al. 2009; Forsberg et al. 2011; Sun et al. 2008). In the presence of a surface texture, multiple wetting states are possible that are distinguished by the degree to which the fluid penetrates into the recesses of the texture. The two wetting extremes are the Cassie–Baxter state and the Wenzel state. In the Cassie–Baxter state, the liquid does not penetrate into the texture. The reduced liquid–solid contact area reduced the apparent solid/liquid interfacial energy and increases the apparent contact angle. In contrast, liquid has lower apparent contact angle in the Wenzel state because it fills all of the recesses. Although the two wetting states can co-exist, there is usually an energy barrier to overcome to transition from one to the other (Koishi et al. 2009). External excitations such as pressure, vibration, thermal energy and electrowetting have been used to overcome this energy barrier (Bahadur and Garimella 2007; Boreyko and Chen 2009; Bormashenko et al. 2007; Forsberg et al. 2011; Krupenkin et al. 2007; Liu et al. 2011b; Manukyan et al. 2011; Ni et al. 2011). Changing the ambient fluid can also initiate wetting transitions (Dhindsa et al. 2006). Textured surfaces not only allow precise control of fluid patterning on the parts and assemblies, but also manipulation of discrete droplets (Shastry et al. 2007; Sun et al. 2008).
- **Electrowetting** is an electromechanical phenomenon where an electric field applied across a fluid interface changes the equilibrium contact area of a droplet on a substrate (Jones 2005). Electrowetting is a powerful method to manipulate fluidic interfaces that is also reversible. While it does not change the actual surface energy, it does change the apparent contact angle and equilibrium shapes. The apparent contact angle decreases with increasing voltage (DC or AC) until it reaches a limiting saturation voltage. Most commonly, it is used with a dielectric layer between the fluid and the electrode [Electrowetting on Dielectric (EWOD)] to reduce electrochemical reactions (Mugele and Baret 2005; Nelson and Kim 2012). Electrowetting applications have been demonstrated in optics, medical

diagnostics, displays, and cooling (Mugele and Baret 2005; Jones 2005). While it is typically characterized by contact angle, it can also be characterized by capacitance (Verheijen and Prins 1999) or force measurements (Crane et al. 2010).

5.1 Droplet positioning and actuation

Multiple steps are needed in directed assembly processes. Parts have to be grasped, moved to the desired location, and then released. Finally, a bond has to be formed between the parts. Capillary force is a versatile tool which can perform all of these tasks.

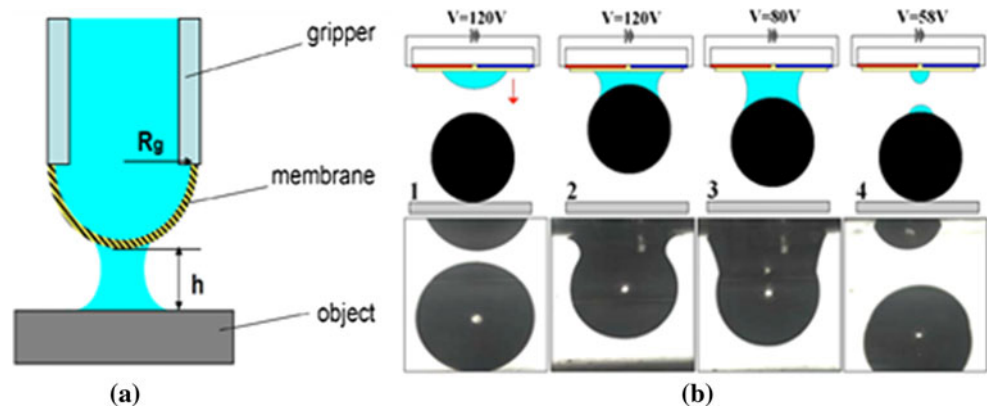
5.1.1 Grasp and release

As discussed above, grasp and release assembly encounters many difficulties at the microscale. Replacing mechanical grasping with capillary grasping can overcome many of these limitations. A droplet can easily grasp microscale parts using surface tension and Laplace pressure. Also, the gripper is not confined by the part's geometry. More importantly, the actuation force can be controlled by the size of the droplet so the gripper will not damage fragile parts. Lambert and Delchambre (2005) studied the capillary gripper design parameters including surface tension, part geometry and grasp/release strategies. Biganzoli et al. (2005) demonstrated a capillary gripper using hydraulic pressure and an elastic membrane. In their study, grasping was achieved by depositing a droplet on the part. A micro-syringe tip with an elastic membrane on one end was brought into contact with the drop (Fig. 6a). Part release was accomplished by increasing the pressure inside the syringe tip. Vasudev and Zhe (2008) used electrowetting to manipulate the gripping droplet. In their experiment, a droplet was suspended from an EWOD substrate, and a voltage potential was applied before the droplet contacts the part. The part was grasped as it was wetted by the droplet. The voltage was then decreased to reduce the grasping force and release the part (Fig. 6b). The same principle is also applied using ionic liquids for high temperature and vacuum applications (Zhe et al. 2011).

For microscale assembly, capillary grippers can be more cost effective than traditional mechanical grippers. However, the release of parts can still be challenging for capillary micro-gripper as the wetting process is not completely reversible. The performance of these grippers could be improved by incorporating additional methods of modulating the capillary forces as described above.

Another type of fluidic micro-gripper uses thermal energy to freeze the surrounding fluid for grasp and release. Yang et al. (2008) cooled the gripper tip with low

Fig. 6 **a** Capillary gripper with an elastic membrane (Biganzoli et al. 2005). **b** Electrowetting-operated gripper (Vasudev and Zhe 2008). Reprinted with permission



temperature gas to nucleate ice and form a solid bond between the tip and the part. Lopez-Walle et al. (2008) created ice bonds at the gripper tip to capture and release a micro part ($0.6 \times 0.6 \times 0.1$ mm) in an aqueous environment using a thermo-electric cooler.

A very intriguing example of using capillary force to grasp and release parts is demonstrated by Hu et al. (2011). In their experiment, an air bubble was introduced into a fluidic environment, and a laser is focused onto the air-liquid interface. Thermal-capillary flow generated by the laser causes the bubble to follow the laser. Microbeads can be either pushed or pulled by the bubble.

5.1.2 Alignment

As part size decreases, the positioning accuracy requirements increase and the cost of “grasp and release” assembly often grows. One solution is to mechanically position parts near the desired location and then utilize a second method for fine positioning. Capillary force is a promising fine-positioning method because it has a clear minimum energy position. Additionally, it can operate at many sites simultaneously.

Originally developed by IBM in the 1960s, surface-mounted technology (SMT) is a widely employed industrial process that uses capillary force for integrated circuitry assembly. SMT technologies such as flip chip (FC) and ball grid array (BGA) places solder paste or small balls (bumps) of solder on the interconnects and then heats them to reflow the solder. The interconnects are designed so the solder wets the metal only. During solder reflow, solder surface tension aligns the mating contact pads achieving accuracies in the micrometer range (Lu and Bailey 2005; Nasiatka and Karim 1995). The large numbers of solder bonds average out the variations in individual bonds in a type of capillary analogy to elastic averaging. The static capillary forces are commonly modeled using the software Surface Evolver (Brakke 1992, 2008; Greiner et al. 2002; Harsh and Lee 1998). Knuesel et al. (2012) reported recent progresses in using solder based fluids to align and self-assemble solar cells. For a more detailed review on flip chip technology and

fabrication techniques, see references (Krishnamoorthy and Goossen 1998; Puttlitz and Totta 2001; Zenin et al. 2011).

In optoelectronics, one key aspect of the fabrication process is the alignment of components for improved performance—whether it is the optic fiber to the wave guide or the optical chip to the electronic chip. In the case of aligning optical fiber to the wave guide, Wale and Edge (1990) achieved alignment accuracy of 1 micrometer in the early 90s. High precision V-grooves are etched into the silicon first and the optical fibers are inserted into the grooves. Solder is then placed on the contact pads. Finally, another substrate which contains the wave guides is mated with the one with optical fibers. Hayashi (1992) investigated the long-term stability of the alignment accuracy of optical chips. He found a variation of less than $0.5 \mu\text{m}$ after 1,000 h (over 300 thermal cycles).

A fluid–fluid interface can also align parts that are too small to grasp. Salalha and Zussman (2005) showed that gold nanowires with $0.5 \mu\text{m}$ diameter and $5 \mu\text{m}$ length can be aligned to the bottom of a microchannel using a fluid–fluid interface through thermocapillary flow. In a similar study, Katz et al. (2006) also aligned rod-shaped bacteria (length $\sim 2\text{--}6 \mu\text{m}$) using the advancing contact line motion of a single droplet.

5.1.3 Bonding

Aside from SMT chip bonding, other liquids and/or ambient fluids are also used for temporary and permanent capillary bonding between parts (Srinivasan et al. 2001). The effect of the composition of both the bonding alloy and the ambient fluid was studied by Morris and Parviz (2008). They concluded that molten alloy works well with parts down to $40 \mu\text{m}$ size scale. Batch assembly of 5,000 micro-sized parts ($40 \mu\text{m}$) was successfully accomplished within 2.5 min. The bonding and alignment forces were sensitive to the volume of the fluids (Greiner et al. 2002). However, a combination of capillary bonding with physical alignment features can be used to improve the accuracy (Ramadoss and Crane 2008; Zheng and Jacobs 2006).

Most of these methods require the deposition of fluids before assembly—limiting the ability to control assembly sequence and uniquely bond particular parts. Jiang and Erickson (2011) developed an alternative method in which fluid interface was created in situ. In their study, a bubble was generated by focusing a laser on a free floating tile. The capillary force between the bubble and the surrounding liquid latched the tiles and a planar structure was built inside a chamber (Fig. 7). This method permitted the assembly of a variety of structures from simple building blocks.

5.1.4 Folding

Folding is a special case of assembly in which a single object is reconfigured by actuating on one or more degrees of freedom in the object. While this is sometimes considered a self-assembly process, the initial connections between the parts reduce the potential errors and speed up the process comparing to self-assembly processes that do not have any initial connections. Additionally, folding processes leverage the substantial body of techniques for planar fabrication to make functional 3D objects. To actuate parts along limited degrees of freedom, fluids can not only provide a micro-gravity environment, but the fluid itself can also be used as an actuator or even a ‘hinge and lock’ mechanism. Originally developed by Syms and Yeatman (1993), folding of a planar template into three-dimensional structures has numerous applications in microfabrication. Demonstrations include microscale inductors and capacitors (Dahlmann et al. 2001; Harsh et al. 1999a), precise 3D alignment of blades for a micro rotary fan (Linderman et al. 2002), and a self-folding/unfolding capsule to deliver drugs or cells (Fig. 8d) (Azam et al. 2011). Furthermore, a tissue scaffold could be folded to provide the building block for “bottom up” assembly of living cells (Fig. 8e) (Jamal et al. 2010; Randall et al. 2012). Conventional folding techniques

include applying thermal energy to a memory alloy; introducing stress to thin films and via external force fields such as magnetic and pneumatic (Leong et al. 2010).

Two different capillary approaches are commonly used. The first uses the surface tension of a droplet to fold a thin elastic membrane (elasto-capillarity or Capillary Origami) (Fig. 8a) (Guo et al. 2009; Py et al. 2007). The elastic substrate can be designed to have different final shapes (spherical, cubic or square). When a droplet of water contacts the substrate, surface energy overcomes bending energy of the elastic sheet and spontaneously folding take place.

The second folding technique, which is more common in MEMS fabrication, involves a material (solder, glass or polymer) that goes through a phase transformation from solid to liquid. Usually, substrates with desired feature are processed by surface micromachining—planar parts with overhang or suspend structures—with or without hinge. Solder is deposited during the surface micromachining processes. Heat is applied to reflow the solder. When in the liquid state, the minimization of free energy from the solder causes planar parts to rotate out of plane to form 3D structures. The rotating torque can be specified by a combination of the amount of solder used and the wettable area on the substrate. Other constraints can also be introduced by adding additional limiting mechanism (Harsh et al. 1999b; Syms 1999; Syms and Yeatman 1993). An additional releasing step can be performed to create free-standing 3D structures (Brittain et al. 2000; Gracias et al. 2002). For example, Harsh et al. (1999a) demonstrated folding of a thin plate with limiting kick stands (Fig. 8b). Azam et al. (2011) created all polymer containers with windows for bio-applications (Fig. 8c). Capillary force has the advantage of easy fabrication using lithography, and the potential to sequence folds using different chemical, thermal triggers and/or gradients. Much effort has been devoted to surface tension-enabled self-assembly including micro-fabrication,

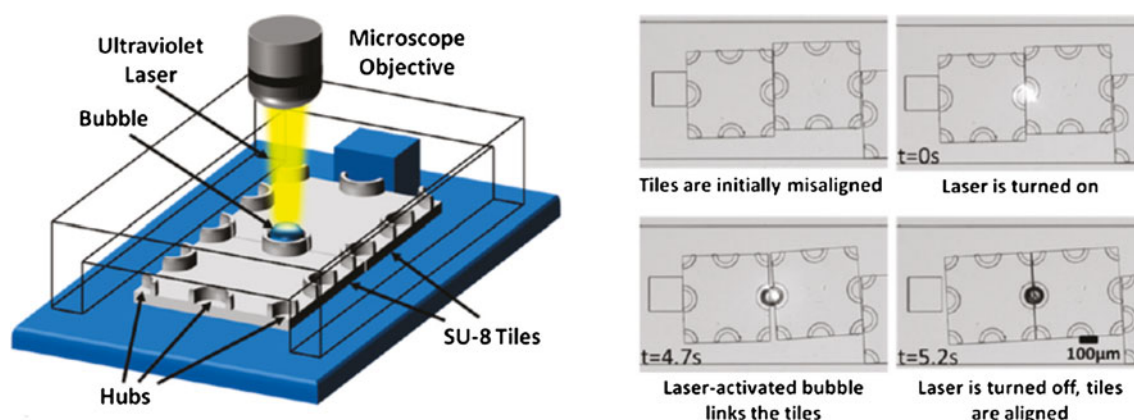


Fig. 7 A laser locally heats the material to a bubble (left). The surface energy of the bubble interface can align and connect SU-8 tiles (right). Reprinted with permission from (Jiang and Erickson 2011)

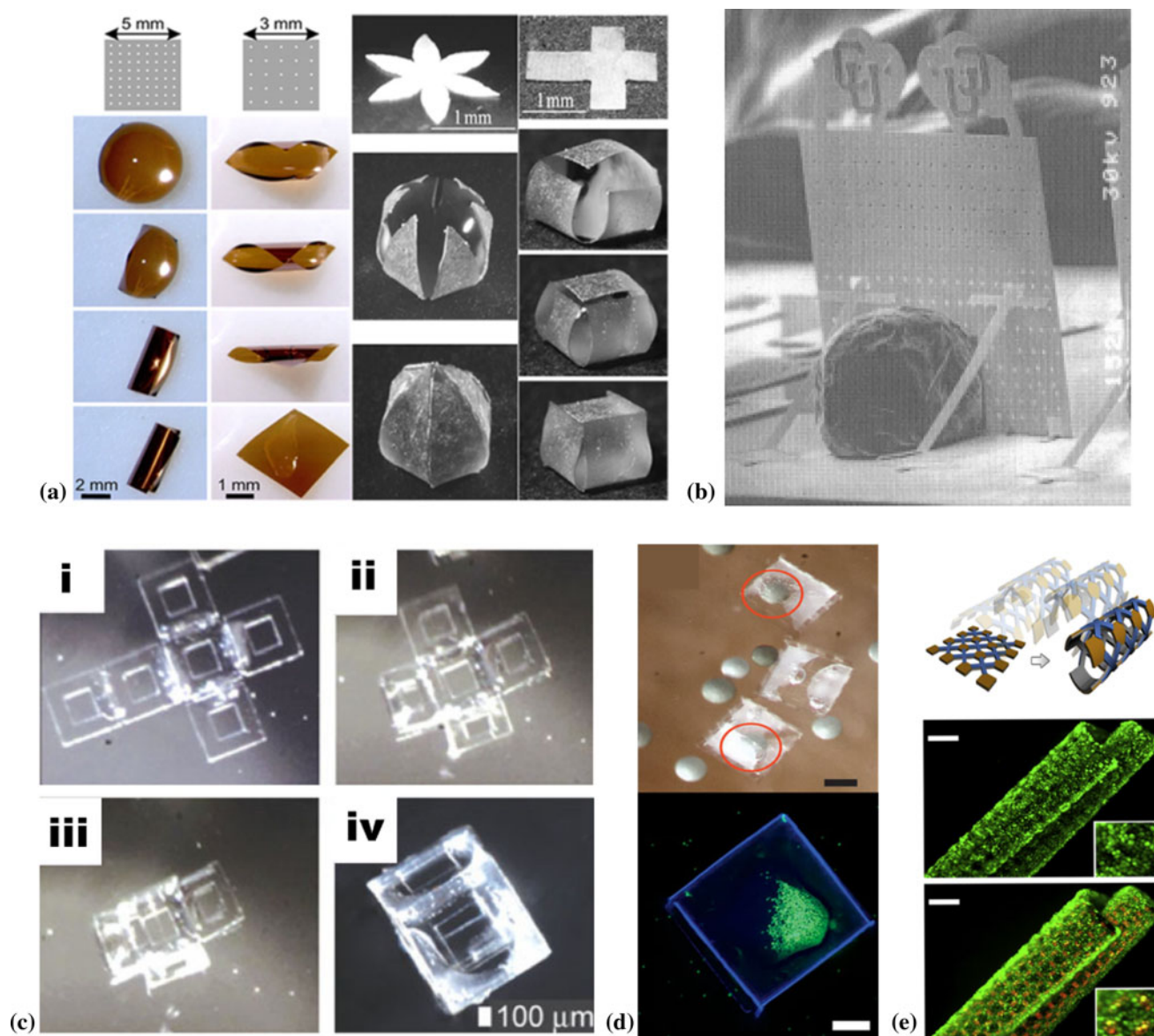


Fig. 8 **a** Varies shapes of elasto-capillary folding (Guo et al. 2009; Py et al. 2007). **b** Solder assembled MEMS with kickstand (Harsh et al. 1999a). **c** All polymeric container self-folding (Azam et al. 2011). **d** Container encapsulating *Artemia* eggs (top) and fibroblast

cells (bottom), scale bars are 250 μm (Azam et al. 2011). **e** Bio-scaffold self-assembly (top) and fluorescently stained fibroblasts cultured on a cylindrical scaffold with its growth progression, scale bar is 200 μm (Jamal et al. 2010). Reprinted with permission

modeling and applications, which are beyond the scope of this article. For a more detailed review, see ref (Syms et al. 2003).

5.2 Interfacial positioning and actuation

The methods described above utilize droplets that are of similar dimensions to the parts or smaller. Below are several methods that use capillary force on an interface to position and actuate parts/objects. In these cases, the interface is much larger than the parts. The processes show particular potential for programmability and directionality.

Many assemblies take place at an interface. Traditionally, this may be a solid interface such as the surface of a table. However, at the microscale, surface tension can support objects at a liquid interface. Deformations of the interface due to the object buoyancy, wetting properties of submerged objects, and/or external inputs can be used to actuate objects on the surface. When parts are placed on a fluid–fluid interface, lateral capillary force arises due to the curved interface. Two classic scenarios are illustrated in Fig. 9. When gravity causes the interface to deform, it is defined as “flotation force” (Fig. 9a). When curvature of the interface from the wetting properties of the parts

deforms the interface, an “immersion force” (Fig. 9b) is created.

Minimization of the free energy on the interface results in an attractive/repulsive force between the parts. Parts that cause the same surface curvature experience an attractive force while parts with different surface curvature are repelled. Drawing an analogy to the Coulomb’s law, a “capillary charge” can be introduced to approximate the attractive/repulsive force between part/body (Kralchevsky and Nagayama 2001). The force (F) is

$$F = -2\pi\gamma \frac{Q_1 Q_2}{L} \quad (2)$$

where γ is the interfacial tension, Q_1 and Q_2 are the capillary charge, and L is the separation distance. Detailed derivation of the capillary charge Q can be found in (Kralchevsky and Nagayama 2001). The scaling of these two force types with part size differs because of their different physical origins. For spherical parts with radius of R , the floatation force $\propto R^6/\gamma$; and the immersion force $F \propto R^2/\gamma$. As the size of the parts decreases, the floatation force reduces at a much faster rate than the immersion force. For particle size less than $5 \mu\text{m}$, the floatation force is usually negligible.

The “assembly by shape” method utilizes above-mentioned attractive force to assemble three-dimensional parts in space. Different wetting properties can be specified and parts on the interface can self-assemble accordingly (Fig. 10a, b). Clark et al. (2002) assembled hexagonal shaped plates into a template. Bowden et al. (2001) assembled chains on a fluid–fluid interface (Fig. 10a). Zamanian et al. (2010) showed that different shapes of microgel can be shaped into a tissue-like structure assembled chains on a fluid–fluid interface (Fig. 10a). Most often, shape assemblies are done in a batch process; the wetting properties of the parts determine the process. But there are also other methods that can be applied to control the curvature of the interface to achieve directed assembly process. Crane et al. (2011) used electrowetting to alter the surface curvature and moved individual parts along desired path, as illustrated in Fig. 10c, d.

Parts can also be moved along a solid surface by attaching them to individual droplets. This approach builds on the techniques of digital microfluidics that have received particular attention in the area of medical diagnostics. Several examples have been published using electrowetting. Moon and Kim (2006) demonstrated a liquid conveyer system in which four droplets carried a thin glass plate (Fig. 11a). Nelson et al. (2011) developed a continuous electrowetting method which eliminated multiple electrodes to reduce the fabrication and programming complexity. This technique could be readily applied to the actuation of solid objects over long distances. Crane et al. (2011) demonstrated the idea with a $9 \times 9 \text{ mm}$ glass plate carried by a droplet (Fig. 11b). These techniques could form the basis of microscale conveyors and positioning systems for assembly.

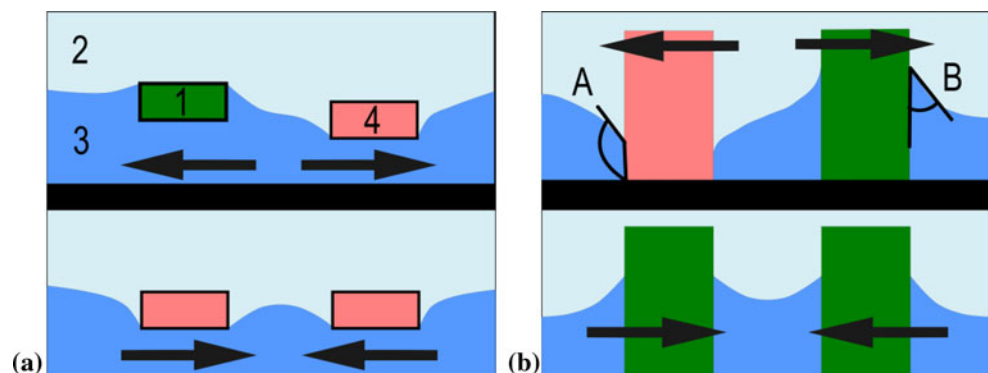
6 Assembly via viscous forces

The advantages of fluid-based assembly systems have been discussed above. Additionally, capillarity has been reviewed as an assembly mechanism. This section will review the use of fluid pressure, shear forces, and fluid manipulation techniques for microscale assembly.

6.1 Characteristics of systems based on fluid forces

Design for microscale fluid–solid interactions has different conditions and limitations than at the macroscale. For example, buoyancy forces significantly diminish the effects of gravity and friction, which tend to restrict motion of microscale bodies. Due to the large surface area, drag forces become more significant. Additionally, the ability to create complex microfluidic systems with integrated valves and pumps facilitates complex fluidic processes. Fluid viscous forces also offer flexibility on material selection. Desired functional properties (such as magnetic and electrical affinities) do not conflict with fluid-driven assembly process. Viscous forces primarily considered here are most sensitive to size, shape, and density of the microscale components.

Fig. 9 **a** Capillary floatation force where the density $\rho_1 < \rho_2 < \rho_3 < \rho_4$. **b** Capillary immersion force. Adapted from Kralchevsky and Nagayama (2001)



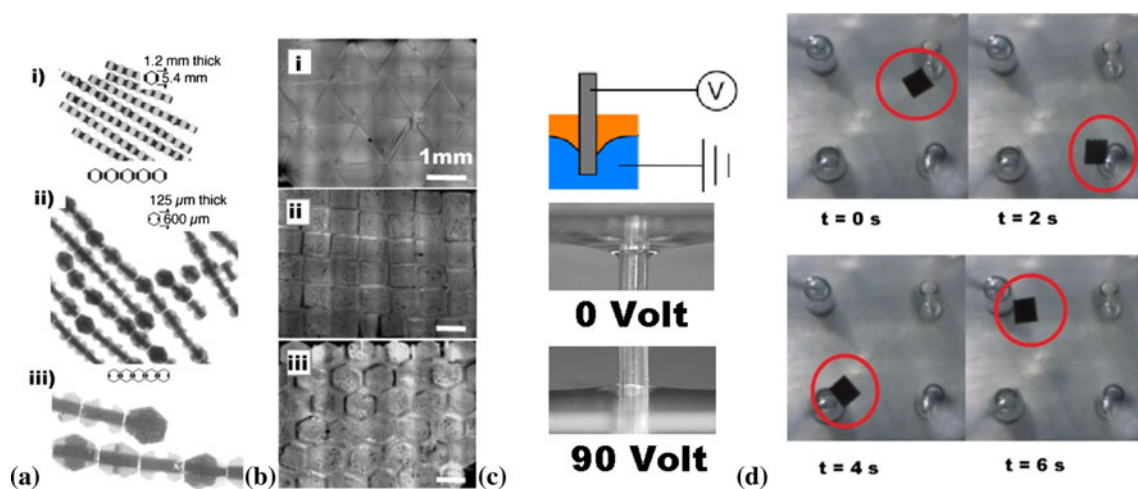
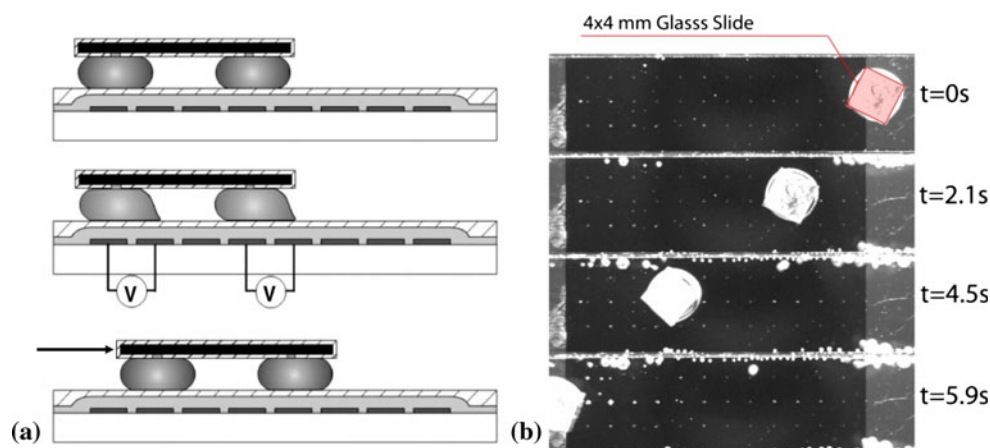


Fig. 10 **a** Pre-specified wetting properties drive assemblies into chains, the *dark sides* are hydrophobic and *light sides* are hydrophilic (Bowden et al. 2001). **b** Close-packed assemblies of triangular, square, and hexagonal shaped microgel parts at fluid/fluid interface (Zamanian et al. 2010). **c** Electrowetting can be used to change

curvature around hydrophobic metal rods (Crane et al. 2011). **d** 4 mm square plate floating on a water/hexadecane interface is moved between four rods according to the voltage applied to the rod (Crane et al. 2011). Reprinted with permission

Fig. 11 **a** Electrowetted droplet moving a glass plate (Moon and Kim 2006). **b** Continuous electrowetting carrying a 4 mm square glass (Crane et al. 2011). Reprinted with permission



Several studies have combined fluid forces, with other manipulation techniques. The fluid forces provided gross positioning after which other forces provided fine motion for final placement and alignment. Singh et al. (2005) employed a pipette method to transfer a fluid dispersion of assembly components onto an assembly sites substrate. A solid mask helped to physically guide the components towards the assembly sites. Assembly sites were recessed, and their shape matched that of the incoming components. Fine alignment was promoted by agitating the system with fluid shear forces, and allowing for components to fall, by their own weight, into place. Srinivasan et al. (2001) used the pipette method for transporting parts, and then capillary forces to generate bonding. Staath and Parviz (2006) showed how fluid flow carries precursor parts across assembly sites, until capillary forces provided bonding.

Besides providing gross motion, fluid forces can also facilitate stochastic-based processes through agitation, by providing large numbers of part–site interactions. Stochastic-based processes rely on these interactions to obtain high assembly yields. Verma et al. (1995) used fluid buoyancy and fluid flow to recover non-assembled parts, hence recycling part–site interactions and enhancing process yield. Several studies relied on fluid agitation (Jacobs et al. 2002; Soga et al. 2003; Zheng et al. 2006; Zheng and Jacobs 2004) and Marangoni flows (Morris and Parviz 2006) to enhance the number of favorable interactions between binding surfaces in SA.

6.2 Assembly with microfluidic technology

At the macroscale, object conveying and sorting has been done with fluidics (Gluskin 1970), but it is not practical in

many applications. However, at the microscale, microfluidic devices provide a wide variety of microfluidic techniques for particle sorting applications. See, for example, (Zhu and Nguyen 2010). Sorting could be viewed as a gross-positioning step in assembly processes, by bringing a disordered dispersion of components into a desired arrangement. Therefore, current techniques for sorting particles and immiscible fluid droplets could be applied for assembling precursor components instead. While these are often spherical components, methods are available to sort components with orientation control. For example, railed microfluidic channels were employed for orientation-based sorting of pre-fabricated components (Park et al. 2009).

Besides sorting components, microfluidic channels have been employed for aligning assembly precursor components. Many macroscale assembly processes address part-alignment during part-transport. Concurrent transport and alignment allow for simplifying an assembly process, and increasing production rate. At the microscale, microfluidic channels can be used as an assembly line conveyor. Fluid flow can collect parts from a disordered array into a microfluidic channel. A channel's physical confinement allows for aligning conveyed components in a desired way, while fluid forces provide source for motion. At the end of a channel (or conveyor), assembly can then begin with oriented components.

Dendukuri et al. (2006) employed a microfluidic channel as an assembly line, based on stop-flow lithography method. A flow of a photo-curing polymer was exposed locally to external UV light. The resultant solid objects of pre-defined geometries were conveyed, and then assembled, via fluid-motion into aggregates of simple geometries. As a complement to a stop-flow lithography system, Chung et al. (2008) designed microfluidic channels with rail-features that constrain component orientation. Rails within a microfluidic channel can remove all but one degree of freedom. Another study applied this mechanism into 3D assembly (Chung et al. 2011). There are limitations, however, in geometric complexity and material diversity in this process. For example, component design must include features that make a component fit into a railed channel.

Assembly has also been performed within microfluidic channels themselves. Vanapalli et al. (2008) demonstrate how spherical particles (of few tenths of μm in size) are assembled into ordered chains. Particles are fed through a microfluidic channel up to a confined section along the channel. The confinement is activated by a particular membrane valve design. This constraint is just large enough for only fluid to flow, thus jamming particles within the channel. This causes particles to closely pack into pre-defined structures. The size of the microchannel relative to the particle size determines the packing structure of the assembled particle chains (i.e., angle formed between

particles and unit structure of chain array). Such method can generate desired chain structures, resembling a synthesized polymer chain. Through simulation and analytical modeling, authors demonstrate the feasibility of applying this assembly method at the nanoscale. Potential microscale applications may include assembled components, delivered in the form of dispersions, for either direct implementation, or subsequent assembly. Examples of these implementations can be reviewed elsewhere (Huck et al. 1998; Randall et al. 2012).

Microfluidic channels facilitate the use of fluids to exert motion upon solid components. However, component motion is limited to 1D manipulation. Efforts based in microfluidic channels are mostly process-directed strategies. In other words, components are designed around the process, and once they are inserted in the system, there is not much room for reconfiguration.

Microfluidic chambers, on the other hand, have shown capacity for controlling reconfigurable 2D fluid force fields. Schneider et al. (2011) studied laminar flow fields within a microfluidic chamber analytically. Flow fields were defined by the flow status at each inlet and outlet. The number of ports and the relative chamber size directly controlled the number of nodes at which different field vectors converge. These convergence nodes would then provide equilibrium locations for components present within the chamber. See Fig. 12 for illustrations of generated component arrays modeled through this concept.

Tolley et al. (2008) used a microfluidic chamber equipped with several inlet and outlet ports. Systematic use of valves controlled flow through each port individually. This turned the chamber flow field into translation and rotation forces for component manipulation. Figure 13 shows how sequential control of valves would drive a component through several paths, up to a successfully assembled state. Krishnan et al. (2008) have modeled fluid–solid interactions for the above-mentioned system. Component motion was achieved by a combination of pressure and shear forces. While a general flow direction achieved gross motion of the component, orthogonal force vectors achieved fine motions for final component placement. Optimum combination of flow parameters and part geometry were selected for accomplishing successful assembly sequences (Figs. 14, 15).

The approaches discussed above used viscous forces from 2D flow as an assembly tool. In other words, these fluid-driven assembly systems adopted a tool-directed assembly strategy. These efforts are inherently limited in assembly rate, as they are serial (components are assembled one by one). However, complex geometries are achievable if the concept is extended to create more elaborate systems. Assembly components can also be designed with convenient geometries and features, which would enhance process efficiency.

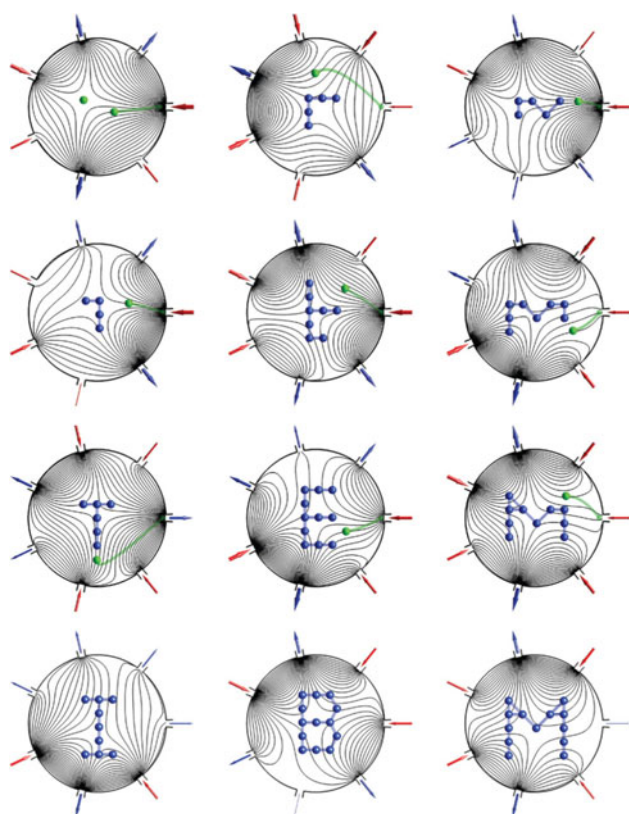


Fig. 12 Model sketches representing controllability of flow fields, capable of arranging solid particles in several configurations (Schneider et al. 2011). Reprinted with permission

Krishnan et al. (2009) have offered a potential solution for a part-driven assembly system, based on fluid forces. Assembly precursor components had internal valves with the ability of guiding fluid flow through. Figure 13e–j illustrates how valves can manipulate component position

and orientation. While a general flow field was necessary for actuating gross motion, valves allowed control of fine motion of each component individually. This work demonstrated assembly through both simulation and experiment. The same strategy was expanded to 3D assembly, yet with much larger components with a few centimeters in size (Kalontarov et al. 2010; Neubert et al. 2010). As described in Sect. 2, part-directed assembly systems have the benefits of being re-programmable, completely deterministic, and requiring no complex fixtures. One drawback was that permanent bonding required secondary mechanisms, such as mechanical latches (Kalontarov et al. 2010; Tolley et al. 2008) and bubble latches (Jiang and Erickson 2011).

The importance of microfluidic valve technology has been evidenced by the above-cited efforts. First, many applications would involve small components, which would require smaller valves. Moreover, remote-control was required for valves inside the components. Such valves imposed a constraint on minimum component size. Current solutions involve thermorheological fluid response for switching flows on and off (Krishnan et al. 2009). When heated, these fluids increase their viscosity considerably. This eliminates the need for additional fabrication steps to form valves. However, this imposes limitations on the environments that can be utilized for assembly.

The above-mentioned examples demonstrate how current microfluidic technology for fluid-flow control is used for component transport, orientation, and assembly. Additionally, a variety of solutions among microfluidic channels and chambers offer a balance between simple part manipulation, and assembly structure complexity. Further development of valve technology and permanent bonding techniques is still needed.

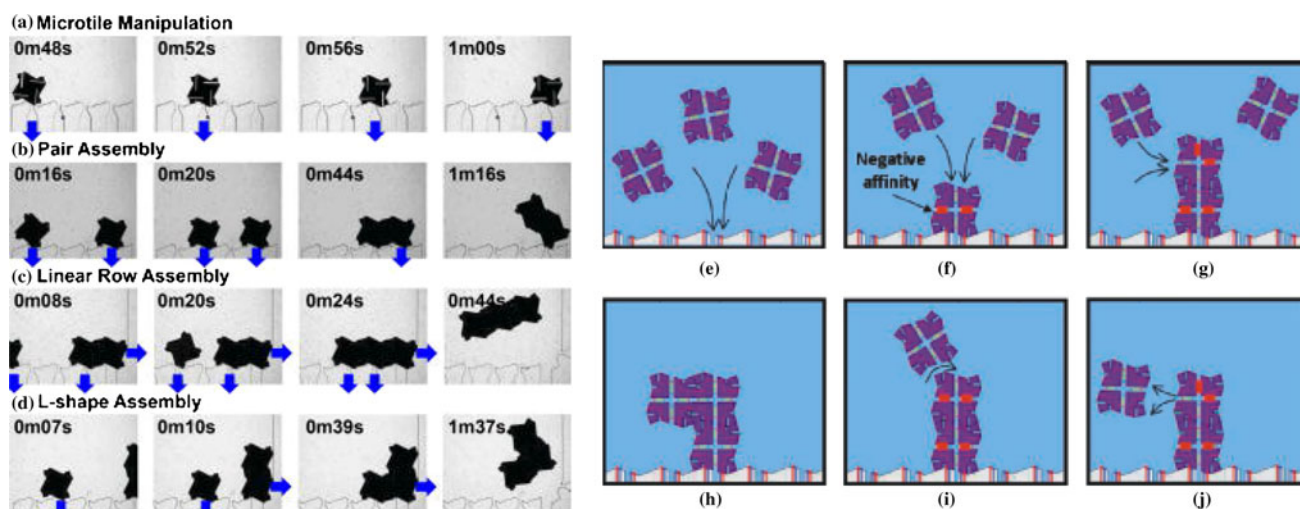
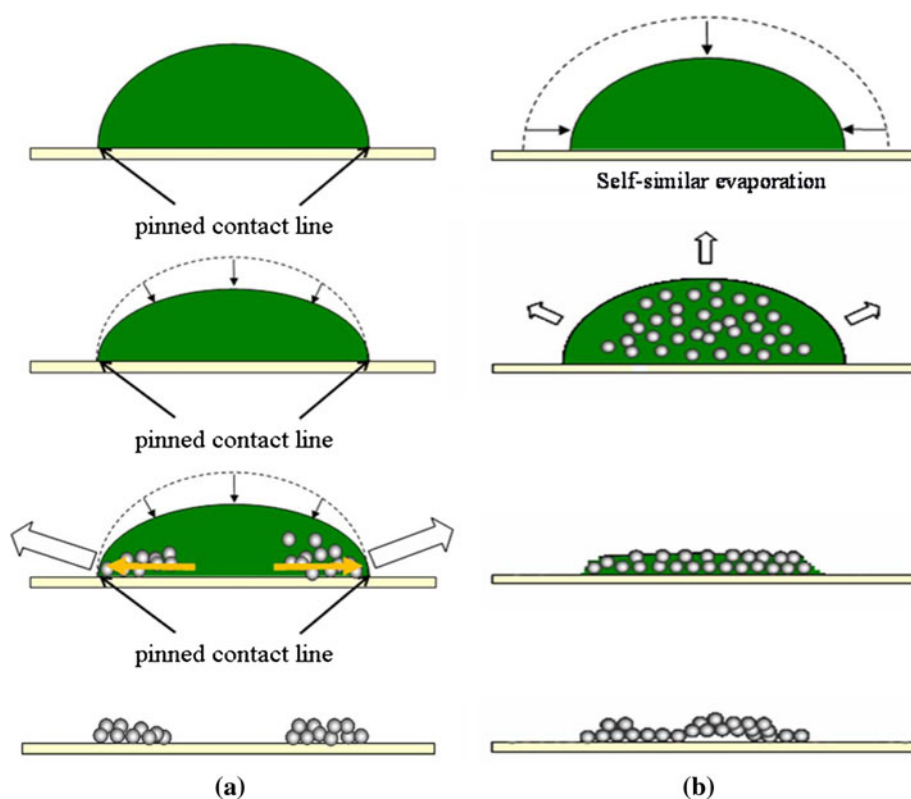


Fig. 13 Microscale, 2D assembly of micro tiles within a microfluidic chamber (a–d) (Tolley et al. 2008). Fluid sinks are created through the outer walls of the chamber, or even through the assembled components (e–j) (Krishnan et al. 2009). Reprinted with permission

Fig. 14 Solid deposit distributions created by evaporation method using different substrate wetting conditions. **a** When contact line pinning occurs deposits concentrate near the contact line. **b** Nonwetting droplet (contact angle $>90^\circ$) favors a more uniform deposit (Joshi and Sun 2010). Reprinted with permission



6.3 Assembly of colloidal particles within microscale fluid bodies

The previous discussion considered the assembly of components submerged in a fluid medium. For these cases, deterministic control of individual objects is possible. Colloidal assembly systems offer a different set of assembly strategies, which are process-directed. The typical particles are of sub-micrometer size and are readily manipulated by fluid flows created by external inputs. While colloidal assembly systems generally offer process-directed assembly strategies, very useful assembly structures can be produced at the nanoscale (Huck et al. 1998; Xia et al. 2000). Colloidal assembly systems can be controlled by relatively accessible inputs to create a variety of structures (Denkov et al. 1992). These systems can be less expensive than currently employed systems.

Among many examples of early approaches to colloidal array deposition include that of Deckman and Dunsmuir (1982), Fisher (1981), and Pieranaski et al. (1983). One strategy for assembling colloidal particles into crystals relies on fluid flow through a fine mesh, which retains the colloidal particles (Park and Xia 1999). Upon retention, particles arrange themselves into a crystal structure. Solvent evaporation has also been investigated for achieving ordered arrangement of colloidal particles. Denkov et al. (1992) have provided experimental rationalization on how capillary forces drive crystalline formation order upon

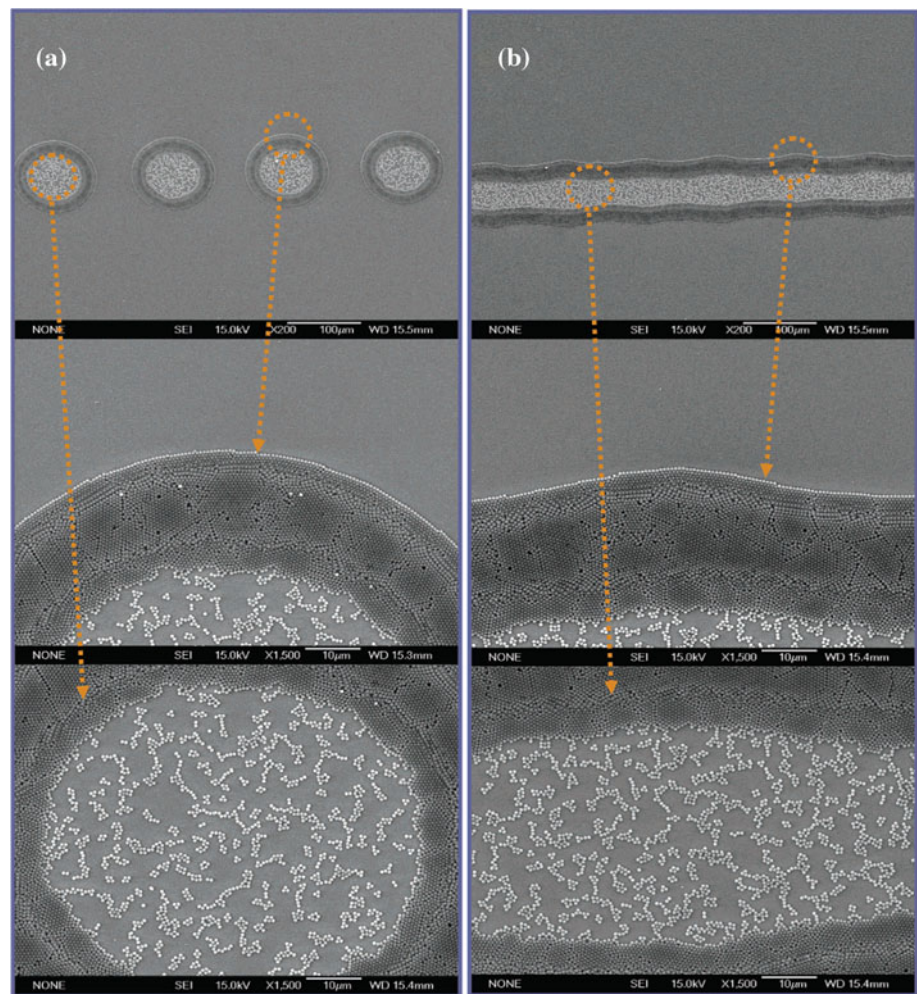
solvent evaporation Deegan et al. (1997, 2000) have provided a comprehensive study for the case of droplets or narrow patterns (e.g., stripes). In this case, internal convective flows transport particles towards the pinned contact line, so that ring patterns, and stripe patterns are naturally formed (Park and Moon 2006).

Colloidal assembly has become attractive because of the various approaches that can control the assembled structures. Dimitrov and Nagayama (1995, 1996) have developed the “Convective Assembly” strategy, capable of forming monolayer and bi-layer (and thicker) crystals, as well as covering large areas ($>1 \text{ cm}^2$). Here, control of the liquid meniscus geometry defines evaporation rate as well as layer thickness. As a result, relatively inexpensive systems can deposit crystal layers with desired parameters, and precise thickness. Control variables of such a system include ambient humidity and temperature, solvent surface tension, substrate–interface alignment, colloidal suspension concentration, particle size and rate of substrate withdrawal. Recent works in convective assembly have achieved additional capabilities. For example, 2D patterns were generated by combining convective assembly with pre-patterned substrate topography (Yin et al. 2001) and surface energies (Bae et al. 2007; Watanabe et al. 2009), and stick–slip motion of the meniscus (Huang et al. 2005).

A different approach, originally called “natural lithography” was first introduced by Deckman and Dunsmuir (1982) and then further developed by Hulst and Van

Fig. 15 Solid particle distribution from ink-jet printed features showing a large concentration at the edges.

a Droplets can generate *ring-like patterns*, with internal nanoscale patterns. **b** Dispensed fluid lines can generate multiple collinear stripes, which also contain nanoscale patterns within (Park and Moon 2006). Reprinted with permission



Duyne (1995) under the name “Nanosphere Lithography”. This method was capable of depositing defect-free colloidal crystal layers over large coverage areas, by using spin coating. The use of spin coating allows spreading a thin suspension film before evaporation, thus allowing for a more uniform particle distribution. More recent efforts have utilized this method for patterning colloidal crystals via pre-processing of substrate surface topography (Xia et al. 2004).

A wide variety of applications have been targeted by colloidal assembly systems (Xia et al. 2000). Recent work has developed the above-mentioned approaches for more specific purposes. Patterning of colloidal crystals have been utilized for data storage (Springer and Higgins 2000; Sun 2000) and as templates for patterning proteins (Yuan et al. 2007). Furthermore, the nanometer size of colloidal particles and the highly uniform crystalline colloidal layers allowed fabrication of optical elements (Dimitrov et al. 1999; Maenosono et al. 1999; Matsushita et al. 2000) and nanoscale lithography masks [reviews on this topic can be found elsewhere (Burmeister et al. 1997)]. Furthermore, 3D growth of colloidal crystals has allowed for fabricating

porous, and composite nano-structures (Velev and Kaler 2000; Velev and Lenhoff 2000), and free-standing 3D structures have been explored (Huck et al. 1998).

Colloidal assembly systems provide a set of strategies, similar to that of nature, for fabricating larger (micro and macro) structures; i.e., building large objects out of extremely small building units. More importantly, as development of colloidal assembly systems matures, hybrid fabrication systems can be designed in order to merge previously incompatible capabilities.

7 External field-mediated assembly

In the previous sections, microscale assembly mediated by fluid forces including capillary, and viscous forces were discussed. This section discusses the assembly processes that take place in fluids, but that utilize non-fluidic forces for process control. Typically, fluids supply critical aspects of the assembly environment such as buoyancy force, reduced adhesion, and electrical insulation. These methods

are tool-directed assembly strategies, but using external field and force inputs rather than physical grippers has many advantages. Directed assembly permits assembly of more complex systems through improved sequence control and fabrication of multiple systems from a single set of parts. There are several types of external fields, forces, and methods reported in the literature; including, but not limited to electric, magnetic, and acoustic fields. These forces can be used for both process-directed (SA) and tool-directed assembly. In some processes both aspects can even be used. For example, long-range forces could be used to achieve gross positioning as a tool-directed strategy. Then a stochastic, SA process driven by short-range interactions could be used for the fine positioning.

This section focuses on external field-mediated fluidic assembly. It also addresses bio-mediated assembly with forces exerted by bacteria swarms that are directed using external fields such as light and magnetic field. In this section, the methods and driving mechanisms of each of these external fields are discussed, and corresponding applications are presented. Additional information on SA processes utilizing external fields is found in review papers by Whitesides and Grzybowski (2002), Morris et al. (2005) and Mastrangeli et al. (2009).

7.1 Magnetically controlled assembly

Magnetic forces have the advantages of non-contact and long-distance action, high-energy density; independence from the medium and the surface chemistry; and favorable scaling at the microscale (Mastrangeli et al. 2009). Magnetic interactions can be attractive or repulsive depending on polarization, magnet geometry and materials. Magnetic forces can be employed in short range (fine positioning) and/or in the long range (gross positioning) for assembly purposes. Short-range magnetic forces, which involve attractive and/or repulsive interactions between individual components, are used to manipulate micro-particles. Long-range magnetic forces, which are usually obtained by strong external fields, are used to manipulate or move particles through relatively longer paths. They are suitable for tool-directed assembly, as both part transport and bonding are achievable. Magnetic forces scale with strength of the magnetic field (either external or components' internal fields), and the volume of the components. Orientation control can be achieved by changing the direction of the external magnetic field (by rotating permanent magnets or multi-coil electromagnets), or adjusting the magnetic characteristics of individual components and/or the shape of the components (Tottori et al. 2011).

Short-range magnetic forces can be used to assemble parts via magnetic interaction between individual parts. A pre-requisite to some magnetic assembly methods is the

assembly of magnetic particles into microscale magnetic domains. Fonstad (2002) and Perkins (2002) were among the first to use short-range magnetic forces for the assembly of hetero-structures on electronic substrates. A short-range magnetic force was utilized in a fluidic medium to position the devices in shallow cavities of the target substrate. A highly magnetic cobalt–platinum alloy was patterned at the bottom of the cavities and magnetized in the direction normal to the substrate. Two different assembly methods were tested. In the first method, the substrate was tilted and vibrated for the particles to fill the cavities where the particles were trapped by the magnetic interaction. In the second method, the particles were sedimented on the substrate, and then the substrate was tilted and topped with remaining unassembled particles repeatedly until all cavities were filled. The assembly was finalized by filling the voids with a polymer followed by planarization. The technique was extended by Shet et al. (2004) with an external magnetic field induced in the substrate accompanying the short-range magnetic forces in the cavities. A continuous oscillatory magnetic field was applied to the back side of the patterned substrate wafer.

The interaction between magnetic objects can also be employed in the absence of an external field with short-range magnetic interactions. Love et al. (2003) demonstrated the use of magnetic interactions between ferromagnetic objects to direct and stabilize the objects in the absence of an external magnetic field (Fig. 16a, b). Lateral assembly of 3D structures was obtained by suspending nickel/gold rods in a solution and applying ultrasonic excitation. Hexagonally close-packed structures were formed. It was observed that, the rods were assembled only side-by-side, rather than more desirable head-to-tail configuration. The side-by-side assembly of small number of components, instead of the preferable tail-to-head assembly was due to insufficient global magnetic dipole.

Magnetic structures can self-assemble into several different geometries. The particles acting as short magnetic dipoles were composed of cylindrical-shaped permanent neodymium–terbium magnets, encapsulated within styrofoam disks (Fig. 16c, d) (Golosovsky et al. 1999). Two-dimensional hexagonal lattices with lattice properties tunable by the external magnetic field were formed. Three-dimensional crystals were successfully assembled by stacking the 2D lattices. Microstructure formation using magnetic nanoparticles and patterned magnetic beads on a commercial CD was presented by Ozdemir et al. (2010). Fe_3O_4 nanoparticles were assembled into cylindrical structures during solvent evaporation. Similarly, linear and spherical assembly of magnetic nanoparticle-loaded microscale hydrogels was also reported (Fig. 16e–h) (Xu et al. 2011b). A static magnetic field generated by parallel sheet magnets was utilized for row assembly and the tip of

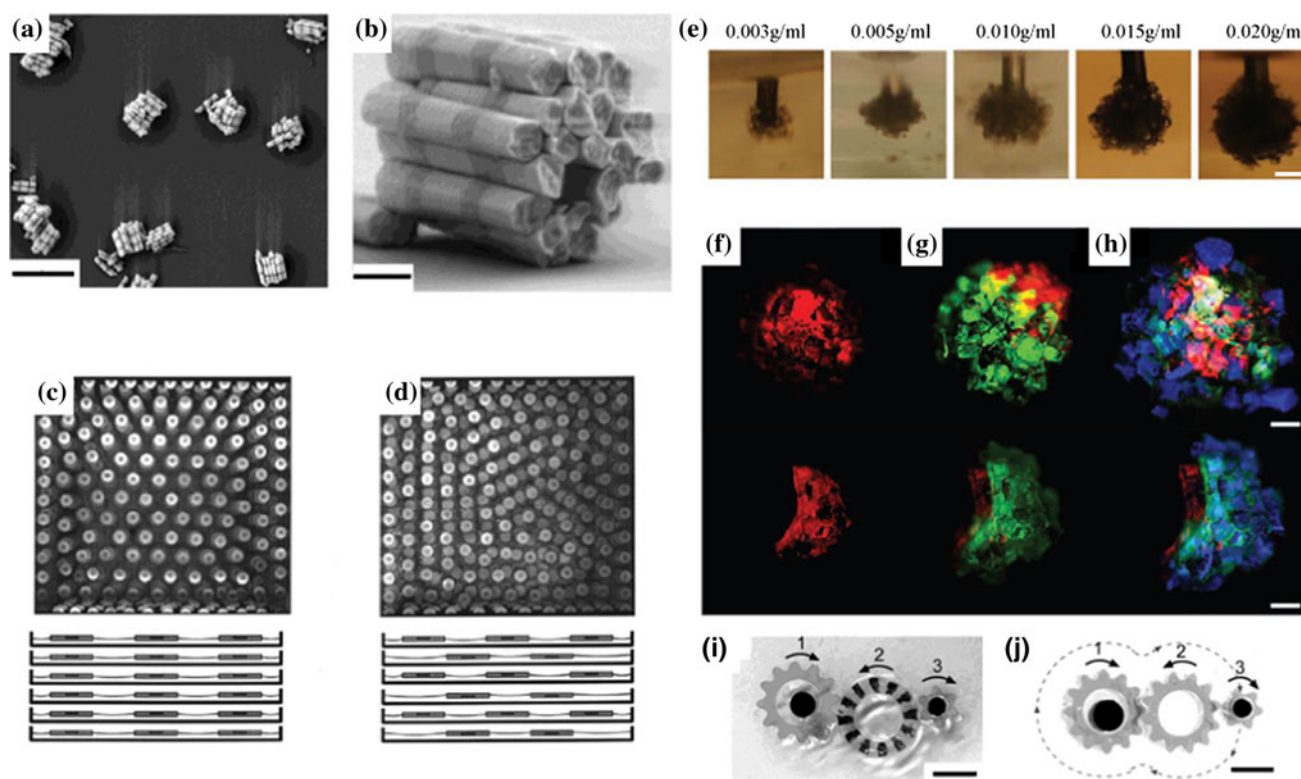


Fig. 16 Various magnetic field-mediated micro-assembly applications: **a** scanning electron micrograph (SEM) of magnetically assembled bundles of rods (Love et al. 2003). Scale bar 5 μm . **b** SEM image of a single bundle demonstrating the alignment of ferromagnetic sections (Love et al. 2003). Scale bar 500 nm. **c** Magnetic particles in a stack of six square troughs in the absence of external field with square ordering at the walls and hexagonal ordering in the middle (Golosovsky et al. 1999). **d** Magnetization direction alternates between the layers (Golosovsky et al. 1999). **e** Multilayer spherical assembly of single-layer microscale hydrogels using five different concentrations (0.003, 0.005, 0.010, 0.015, and 0.020 g/mL). Scale bar 1 mm (Xu et al. 2011b). **f–h** Merged

fluorescent images and cross sections of three-layer spheroids. Scale bar 500 μm (Xu et al. 2011b). **i** Magnetic SA of rotating gears with magnetic and capillary interaction. The schematic diagram shows different types of assembled gears interacting through overlap of menisci. Gears 1 and 3 are hydrophobic and have physical teeth driving the gear. Gear 2 is diamagnetic and does not have physical teeth. The gears are stable in aligned configuration when the linear velocities of the rims do not match, since the interface between the gears allows slip (Ng et al. 2003). **j** Magnetically self-assembled rotating gear mechanical system with gear 2 having teeth, the system does not allow slip. Scale bar 5 mm (Ng et al. 2003). Reprinted with permission

a magnetic rod was used for 3D spherical assembly. Cells encapsulated by the microgels were also successfully assembled in the same study.

Assembly capabilities can be improved by integrating magnetic forces with hydrodynamic effects. Grzybowski et al. reported several magnetic field-driven SA studies utilizing the interactions between magnetic and hydrodynamic effects (Grzybowski et al. 2000, 2001, 2004; Grzybowski and Campbell 2004; Grzybowski and Whitesides 2001, 2002; Ng et al. 2003). Sets of magnetically doped PDMS disks placed on the liquid–air or liquid–liquid interfaces were self-assembled by magnetic forces. The magnetic field was induced by a rotating permanent magnet positioned at the bottom of the beaker. It forced the PDMS disks to spin around their axis at the same angular velocity as the rotating magnet. The relative strength of attractive and repulsive interactions led to the formation of various patterns by altering the number, size and shape of the disks

and the magnet rotation speed. The group conducted several experiments using variants of the setup to further investigate the phenomena associated with dissipative structures, as illustrated in (Grzybowski and Whitesides 2002), including particle shape and vortex interactions, and dynamic SA (Grzybowski et al. 2004; Grzybowski and Campbell 2004; Ng et al. 2003).

Magnetic field-actuated micro-robots permit direct control of programmable assembly, even when the assembled parts are not magnetic. These micro-robots function as assembly tools. External magnetic actuation is effective at the microscale because it eliminates the need to integrate power and actuation mechanisms into a micro-scale mobile device (Diller et al. 2011). The first systems proposed by Gauthier (Gauthier and Piat 2002) and Yesin et al. (2006) relied on field gradients to propel the robots. Wireless resonant magnetic microactuator or micro-robots were later introduced by Vollmers et al. (2008) for

assembly of microscale devices. Based on the proposed magnetic micro-robot concept, microfabrication of the devices and their application were demonstrated as illustrated in Fig. 17 (Frutiger et al. 2009, 2010). Magnetic force-driven micro-robots with control on position, speed and orientation were also investigated. They presented tool-directed assembly with closed-loop control of various micro-objects such as biological entities in aqueous environments on unstructured surfaces. Diller et al. (2011) proposed using submillimeter scale untethered permanent magnet micro-robots (Mag- μ -Bots) which were actuated by external magnetic fields for both assembly and disassembly. They utilized a grid of cells with addressable electrostatic traps capable of anchoring individual micro-robots.

Similarly, an untethered electromagnetically actuated magnetic NdFeB micro-robot was reported by Pawashe et al. (2009). The micro-robots were fabricated by laser cutting of a magnetized NdFeB material. Controllable, varying magnetic fields were induced by a 3D coil assembly. The micro-robot was tested by pivoting the micro-robot about an edge to surmount a non-planar, microscale obstacle. Actuation was demonstrated on several substrates with different surface properties. More recently, rolled Ti/Fe/Pt thin films used as self-propelled micro-robots capable of selectively assembling micro- and nanoscale components were reported (Solovev et al. 2010). Self-propulsion was achieved by ejecting micro-bubbles into the solution by platinum catalytic decomposition of hydrogen peroxide into oxygen and water. The micro-robots were controlled wirelessly by adjusting the external magnetic field. High propulsion power was achieved enabling the transportation of up to 60 particles by one robot. Electromagnetically controlled micro-robots capable of swimming in 3D were also reported by (Yamazaki et al. 2004). Helical micro-robots were demonstrated with applied rotating magnetic fields (Fountain et al. 2010; Kim et al. 2011; Tottori et al. 2011).

Kim et al. (2011) utilized a rotating magnetic field for the spiral swimming micro-robot capable of traveling or swimming in low Reynolds number regimes. The micro-robot was composed of a three-axis Helmholtz coil with a NdFeB spherical magnet, artificial spine, and ribs. The proposed mechanism was based on obtaining a snake-like undulatory and skeletal motion. Tottori et al. (2011) investigated different designs of helical robots with bar-shaped and T-shaped heads with rotating magnetic field to manipulate and orient helical micro-robots. An analysis of torque showed that the torque induced on a helical micro-robot increases with component volume and magnetic field strength. Fountain et al. (2010) demonstrated the use of a single rotating permanent magnet rather than an electromagnet for manipulating helical micro-robots. Most

magnetic micro-robots reported to date were designed for dry applications. However, they can be easily employed in wet assembly; ensuring magnetic field is not affected. Furthermore, magnetic micro-robots can be used in electric field-mediated assembly of more complex systems.

7.2 Electric field-mediated assembly

Static and dynamic electrical fields can easily be induced, controlled and employed for manipulation and assembly of microscale particles/components. Levitation and handling of particles and cells were the first reported applications of using electric field in microscale assembly, with the help of a feedback control systems (Jones and Kraybill 1986; Kaler and Tai 1988). Since its introduction, electric field has been widely used in assembly for various applications. Electric field-mediated assembly will be reviewed under two main branches: electrophoresis and dielectrophoresis.

7.2.1 Electrophoretic assembly

Electrophoresis (EP) utilizes electrostatic fields to manipulate charged particles in liquids of moderate viscosity. EP is widely used in biomedical sciences and microfluidics, and has been proven to be effective in SA of microscopic devices with several successful applications that will be discussed in this section. In the literature, electrophoresis has been employed mostly for SA to form microscale features. Assembly of indium gallium arsenide (InGaAs) and GaAs LEDs were the first reported works for electrophoretic SA in fluids (Edman et al. 2000; O’Riordan et al. 2004). Edman et al. (2000) utilized electrophoresis to assemble LEDs on top of Sn/Pb-coated electrodes. The LEDs were forced to move toward the electrodes with a fluid flow induced by a negative current in the low conductivity fluid. Self-alignment and precise assembly of the LEDs on electrodes were obtained by reversing the current after LEDs were properly positioned on the electrodes. Similarly, an array of electrodes, capable of producing a programmable and switchable electrostatic field was used by O’Riordan et al. (2004) for assembly of mesoscale LEDs. GaAs-based LEDs were precisely manipulated across the array and assembly was achieved at selected electrodes by switching field configurations accordingly (Fig. 18). In both of these LED assembly efforts, the process was finalized by solder reflow to establish metal contacts to the electrodes.

7.2.2 Dielectrophoretic assembly

Dielectrophoresis (DEP) can manipulate and assemble both charged and uncharged particles (as opposed to only charged particle manipulation with EP). In DEP, an object

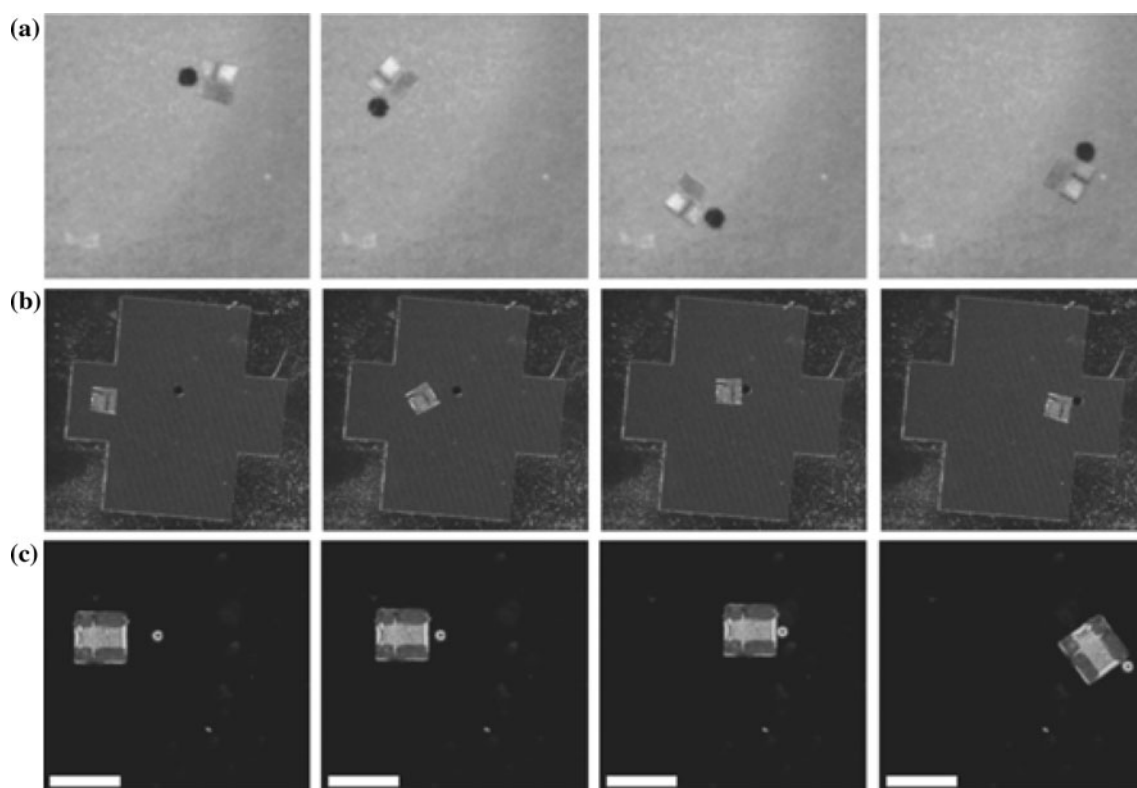


Fig. 17 **a** Magnetic micro-robot image sequences illustrating pushing micro-objects with an asymmetrical 07v6b-MH robot manually pushing a $150\ \mu\text{m} \times 20\ \mu\text{m}$ gold disk over the dry SiO_2 surface (Frutiger et al. 2009). **b** An asymmetrical 07g2-MH robot in a fully

automated operation (Frutiger et al. 2009). **c** Robot of type 07tj-SH is pushing a glass bead about $50\ \mu\text{m}$ in diameter under water over a polished silicon wafer (scale bar is $500\ \mu\text{m}$) (Frutiger et al. 2009). Reprinted with permission

with different conductivity and dielectric constant relative to the fluid medium acts as an electric dipole when a field is applied with charges accumulating at interfacial regions (Mastrangeli et al. 2009).

The idea of DEP was first introduced at early 1950s by Pohl with motion of suspended particles by polarization forces produced by an inhomogeneous electric field (Pohl 1951). The concept was applied to remove solid particles from polymer solutions. Later, it was found out that biological materials such as cells also have different dielectric properties, enabling biological dielectrophoretic manipulation (Pethig 1979). In DEP, the object experiences a force and resulting displacement upon application of a spatially non-uniform, dynamic electric field. The force, is independent of field direction, is proportional to the gradient of the square of the magnitude of the electric field. The components are forced to move towards higher field intensity regions. The object is attracted if its polarizability is higher than that of the surrounding medium (positive DEP); and repelled if it is lower (negative DEP) (Hughes 2000). The direction of the dielectrophoretic forces depends on the dielectric properties of the particle, frequency of the applied field and conductivity of the medium. Particles with different dielectric properties can

be actuated simultaneously in different directions by carefully selecting the component material, the medium, and the electrical frequency.

In positive DEP, the field's energy maxima represent potential minima for the assembling particles. Non-contact manipulation requires closed-loop control, which may be challenging to implement for microscale elements (Mastrangeli et al. 2009). On the other hand, open-loop, non-contact operations are feasible with negative DEP. Rotation of the objects can also be induced with a rotating electric field potentially enabling control of both position and orientation of parts. Several other effects may arise as a result of the rotating electric field such as heat generation leading to electro-thermal forces, convection flow and other electro-hydrodynamic effects. These effects might be favorable or unfavorable depending on the application. Their influence can be comparable with DEP forces for high intensity fields (Castellanos et al. 2003).

Lee and Bashir (2003) used negative DEP and electro-thermal effects for the assembly of microscale silicon resistors between Au/Cr-coated electrodes as illustrated in Fig. 19. The authors also reported self-assembly of $15\ \mu\text{m}$ by $2\ \mu\text{m}$ size, three-terminal silicon metal oxide semiconductor field-effect transistors both by utilizing DEP only,

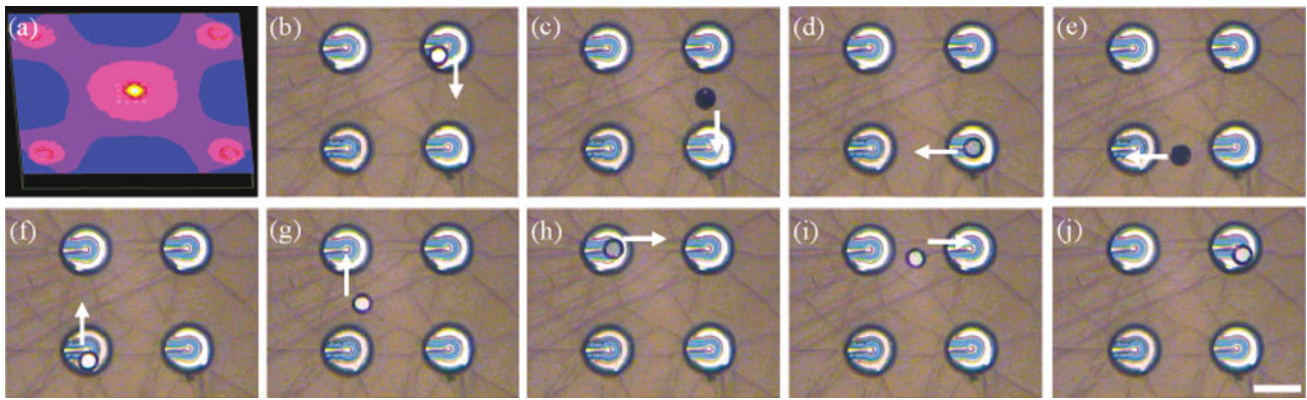


Fig. 18 Manipulation of 50 μm diameter LED using EP: **a** simulation of on-chip electrical field distribution following addressing of a single receptor electrode location versus the counter electrodes. **b** Video image frame of a LED pre-localized at a selected receptor electrode site. **c–j** Video image frames showing that the LED may be

manipulated or “driven” around the receptor array in a programmed manner by sequential electrical addressing of each target receptor electrode in turn. Scale bar is 100 μm (O’Riordan et al. 2004). Reprinted with permission

and with DEP in combination with SAMs of 1,9-nonanedithiol (Lee and Bashir 2005). Negative DEP was used to position particles on top of metal electrodes. Positive DEP between resistors and metals led to assembly. Nonanedithiol was used to improve the stability of the final assembly. Cohn (1997) combined positive and negative DEP, in which a long-range attractive force and a repulsive force at short range resulted in a stable equilibrium at a fixed distance from the electrodes. In the same study, they presented another approach, in which the medium used was a mixture of two liquids with different dielectric constants. The balanced DEP forces levitated the parts at stable equilibrium points. Stable levitation was achieved easily by DEP, but it usually requires a carefully designed standing wave pattern or application of multiple types of external fields using alternative methods. Dielectrophoretic levitation of particles at stable equilibrium points using DEP could be employed for vertical positioning while other type of fields were used for planar manipulation.

A more recent study on electric field-mediated SA on fluid–fluid interfaces was reported by Janjua et al. (2011). Particles trapped at a liquid–fluid interface assembled under an electric field normal to the interface. The field caused dipole–dipole electrostatic repulsion, as well as an electrostatic force normal to the interface. Under these forces, the particles were rearranged to form 2D hexagonal arrays of long-range order and rods were aligned parallel to each other. The method relied on the electrostatic force caused by the change in the dielectric properties at the interface. Because the force increased with the square of the particle radius, this electrostatic force on small particles was more significant than the buoyancy and dielectrophoretic forces.

Nanowire and nanorods (typically microscale in length) are of recent interest due to their exceptional thermal and

electrical characteristics. Nanoparticles and nanowires can be fabricated, assembled and integrated by DEP. For example, Kumar et al. (2009) reported assembly of ZnO nanoparticles into nano-gap electrodes by DEP. They also noted that positive DEP is active at frequencies less than 500 kHz and negative DEP starts dominating at 1 MHz. EP and DEP can be used in the same assembly by adjusting electric field frequency according to the application. The exact frequencies for EP or DEP dominance should be identified either theoretically or experimentally for each application. The time-averaged dielectrophoretic force scaling was noted in this work as shown in Eq. 3, where a is the radius of the particle, $K(\omega)$ is the Clausius–Mosotti factor, E_{rms} is the root mean square value of the electric field, ϵ_p and ϵ_m are the permittivities of the particle and medium, σ_p and σ_m are the conductivities of the particle and medium, and ω is the angular frequency.

$$F_{\text{DEP}} = 2\pi\epsilon_0\epsilon_m a^3 \text{Re}[K(\omega)] \nabla E_{\text{rms}}^2$$

$$K(\omega) = \frac{\epsilon_p - \epsilon_m - \frac{j}{\sigma_p - \sigma_m}}{\epsilon_p + 2\epsilon_m - \frac{j}{\sigma_p + 2\sigma_m}} \quad (3)$$

Burgarella et al. (2010) reported a modular multistage microfluidic platform for selective separation (Fig. 20a), caging (or trapping) (Fig. 20b), focusing (Fig. 20c) and steering cells (Fig. 20d), all based on dielectrophoresis. All of these functions were obtained only by excitation of carefully designed metal electrode array elements with different phase shifts at different frequencies. *Saccharomyces cerevisiae* cells (WBC) and sheep red blood cells (RBC) were used for preliminary experimental verification. The effect of the dielectrophoretic force was clearly shown in Fig. 20a–e, with top and bottom rows corresponding to electric field turned off and on, respectively.

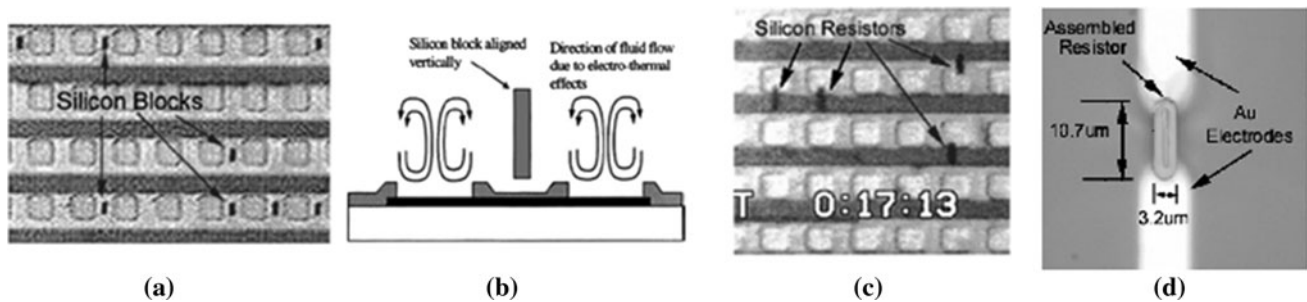


Fig. 19 Use of both negative DEP and positive DEP with the help of capillary effects for assembly of silicon resistors on Au electrodes. **a** Arrangement of silicon blocks vertically on the oxide in between the open windows due to negative DEP. **b** Schematic of the fluid flow lines due to electro-thermal effects leading to alignment of the silicon

blocks. **c** Positive DEP moves the resistors to the contact openings across two adjacent metal electrodes. **d** Close-up of the assembled resistors after the solution is dried (Lee and Bashir 2003). Reprinted with permission

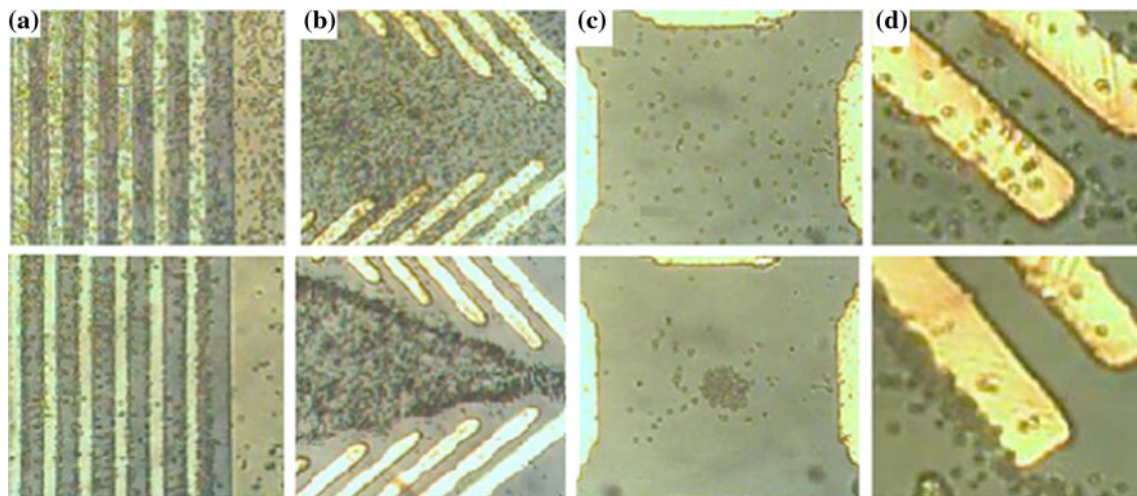


Fig. 20 Modular multistage microfluidic platform for separation, focusing, caging and deviating cells by dielectrophoresis: **a** separation based on cell type by positive DEP of RBC cells. **b** Focusing for

caging. **c** Cell caging using a quadrupole for optical analysis. **d** Steering of WBC cells marked with CD4+ for final separation (Burgarella et al. 2010). Reprinted with permission

Electrophoresis and dielectrophoresis for assembly has a wide design space with the capability for applying attractive and repulsive effects, even simultaneously. The key parameters include electrical properties of components and the liquid, design of electrode geometry and configuration, and frequency of the applied electric field. These effects can be tailored to manipulate, position, and assemble microscale components using only electrodes and applied fields. Orientation control is not easy to achieve in either EP or DEP. Thus, other methods should be employed if orientation control is required. High electrical fields involved may potentially interfere with and damage cells and other biological assemblies.

7.3 Acoustic and vibration field-mediated assembly

Acoustic and vibration fields are easily generated by transducers or actuators in the form of pressure waves in

fluidics. Pressure waves are low power waves (compared with stress waves), which can be used when the components of the assembly are sensitive to electrical charges or magnetism. Pressure wave fields can be formed easily by coupling the fluidic environment with bulk piezoelectric transducers, surface acoustic wave devices, and vibration modes (or mode shapes) of vibrating surfaces. They can be used to levitate or manipulate single components, or they can be used to generate standing wave patterns to manipulate groups of components in the nodes and antinodes, depending on component properties such as size and density (Guldiken et al. 2012).

Structural mode shapes are frequently used to control micro-assembly patterns. They are easy to form by vibrating structures at specific resonant frequencies to obtain specific mode shapes. For example, microscale hydrogels were assembled by acoustic excitation as illustrated in Fig. 21 (Xu et al. 2011a). The hydrogels are

capable of encapsulating cells and proteins to create biological assemblies. The microgels and microbeads of various sizes in a droplet were successfully assembled into regular structures when the droplet was excited by a piezoelectric transducer at various frequencies and intensities. The vibrational mode shapes of the liquid droplet were excited, which generated the required acoustic force to assemble particles at the vibration nodes of the droplet, depending on the frequency. While this method can concentrate particles at the nodes, there is no precise control over the number or orientation of particles in each node. Both single- and double-layer structures (with a second assembly on top of the first assembly) were reported in this study. Another application of acoustic field along with vibration on SA of colloidal solution droplets was presented by Rudenko et al. (2010). The assembly was achieved by standing wave patterns of surface acoustic waves. The assembly was controlled by modulating the frequency and intensity of the acoustic wave and by varying the properties of the particles and the solvent. They showed that the smaller particle sizes and higher surface acoustic wave (SAW) frequencies led to assemblies with better defined boundaries.

Standing wave patterns were also used for controlled pickup of micro-particles from a planar surface (Jia et al. 2012). Acoustic radiation forces on particles near a rigid surface were experimentally and theoretically analyzed. Individual silica, zirconium and aluminum particles of $\sim 400\text{ }\mu\text{m}$ size were levitated and transported to desired locations on a substrate submerged in water using acoustic radiation forces in the nano-Newton range. The standing wave field composed of two obliquely incident plane waves and their reflectors were investigated and optimized by varying the size and position of the sound source. Instant particle levitation was observed when a threshold acoustic radiation was reached. The threshold varied with particle size and type permitting independent control. Trapping and manipulation were also possible by using focused ultrasound for particles in microfluidic channels (Jeong et al. 2011) and for droplets on 2D surfaces (Lee et al. 2010a, b). The acoustic trapping forces were investigated theoretically and experimentally by Lee et al. (2010a) for the droplet case and it was reported that the force required for trapping was increased with increasing liquid viscosity, droplet size, and flow velocity.

Faraday waves, which are nonlinear surface acoustic waves, were also employed for fluidic assembly by Park et al. (2011) to assemble Cr/Au particles on a silicon substrate. The assembly was achieved by tilting the substrate for bringing micro-particles in proximity to substrate; thus allowing assembly. Faraday waves were generated at the fluid surface by a magnetic shaker. Bernassau et al. (2011) reported another acoustic particle manipulation

system with an array of heptagon-shaped bulk piezoelectric transducers. The heptagonal array was utilized specifically to get rid of standing wave pattern. The acoustic field was controlled and manipulated by varying the output phases of the individual acoustic elements. They were able to position particles in straight lines with different angles and in heptagons with different morphologies.

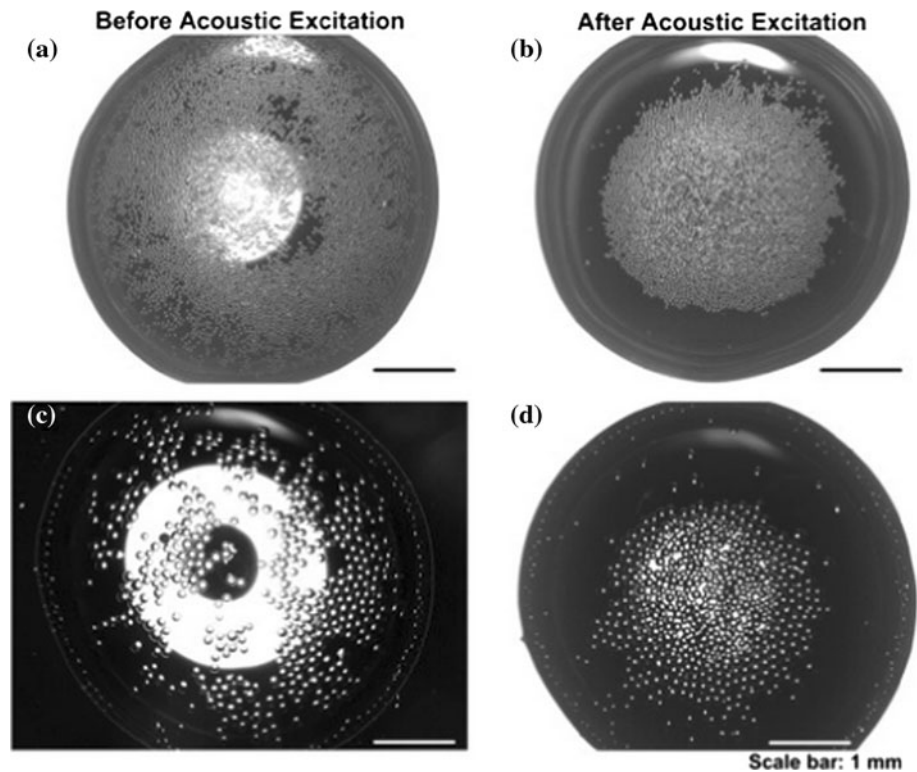
An untethered micro-robot system utilizing both magnetic and acoustic fields was presented by Kwon et al. (2011). Manipulation of a magnetic micro-robot was performed by an external magnetic field formed by an electromagnet array. An $800\text{ }\mu\text{m}$ air bubble was carefully injected into the microchannel, placed just below the micro-robot. After moving the micro-robot next to the $80\text{-}\mu\text{m}$ -diameter glass beads, an acoustic radiation field was applied at the frequency corresponding to the resonance frequency of the air bubble. The excitation forced the bubble to oscillate at its resonance, allowed it to capture the glass bead with surface tension. The captured bead was then manipulated with the magnetic robot. The authors also presented manipulation of an $800\text{ }\mu\text{m}$ fish egg using the same method.

Particle manipulation and handling is relatively easy to achieve by using acoustic fields; however, orientation and position control is a formidable task. The reported advancements to date are primarily stochastic assemblies of part clusters using standing wave fields and mode shapes, with limited control on the assembly. Manipulation of individual particles or components is also feasible, but complex assembly systems and part designs are essential. This necessitates combining magnetic or electric fields with acoustic fields, when more precise control over orientation and position is needed. Acoustic waves can also be highly dissipated or attenuated in propagation, which limits the use of acoustic forces for short-range assembly only, especially for standing SAWs. Even with the aforementioned limitations, the noninvasive nature of the pressure waves and mode shapes makes acoustic fields favorable because they do not electrically or magnetically interfere with components.

7.4 Bacteria swarm assembly

Bacterial swarming is an example of dynamic system in which the interaction of a population of bacterial cells collectively lead to emergent behavior and structures (Copeland and Weibel 2009). It was first developed for microbiological purposes. Bacteria swarm as an assembly tool was first suggested by Martel (2005). Swarm of magnetotactic bacteria (MTB), which respond to magnetic forces, was proposed as the driving force for tool-directed assembly method. The proof of concept of the idea was experimentally performed by manipulation of microbeads attached to the MTBs in an aqueous medium with externally applied magnetic field as illustrated in Fig. 22

Fig. 21 Acoustic assembly of microbeads. Images of **a** distributed 50 μm microbeads before acoustic excitation, and **b** after acoustic excitation. Images of **c** distributed 100 μm microbeads before acoustic excitation, and **d** after acoustic excitation. Bead concentration was 50 mg/mL (Xu et al. 2011a). Reprinted with permission



(Martel 2006). An open-loop control mechanism was employed with optical monitoring. The method was then employed to assemble pyramid-like structures from SU-8 microbeads. The swarm was composed of $\sim 5,000$ MC-1 flagellated bacteria, to which the microbeads were attached (Martel and Mohammadi 2010).

Flagellated bacteria swarms, directed by ultraviolet light were also reported for directed assembly of microscale components (Steager et al. 2007). *Serratia marcescens* bacteria inoculated on an agar plate were used as the swarm to manipulate triangular micro-structures with 50 μm edge length. The motion of the bacteria swarm was controlled externally with optical feedback. The bacteria translation was stopped by local UV exposure and continued upon turning off the UV source.

Bacteria swarm-mediated assembly is a relatively new and promising tool-directed assembly technology, which will potentially gather more interest especially for biological assemblies. Bacteria with possible attachment of various proteins, cells, tissues and inorganic components can be manipulated without necessitating external power input, which is especially attractive where power transmission is a problem.

8 Future of microfluidic assembly

Fluidic media, along with fluidic, and non-fluidic forces have proven to be very effective for the assembly of

microscale devices. Many types of assemblies have been created with a wide variety of methods. While there will certainly be new assembly methods; the more critical area of progress is in increasing the capability of current methods.

8.1 Key challenges

In comparing the mature processes used for macroscale assembly to current capabilities at the microscale, developments are needed in key areas such as

- *Part orientation control* Many processes have little or no control over the orientation of the assembled parts. However, assemblies often require functionally asymmetric parts that must be oriented in particular ways.
- *Increased part variety* Most current assemblies use 1–5 different types of parts, often in repeating arrays. Functional systems will require the integration of more parts.
- *Assembly sequence control* Multipart assembly usually requires components to be assembled in a certain order. Several strategies have been (or are currently being) developed, such as shape matching, and the use of sequentially activated bonds. While these techniques are effective solutions for some cases, they are too complex for other cases. Closed-loop control systems could become ideal solutions for this issue.
- *Functional connections between parts* Current assemblies produce predominately structural connections

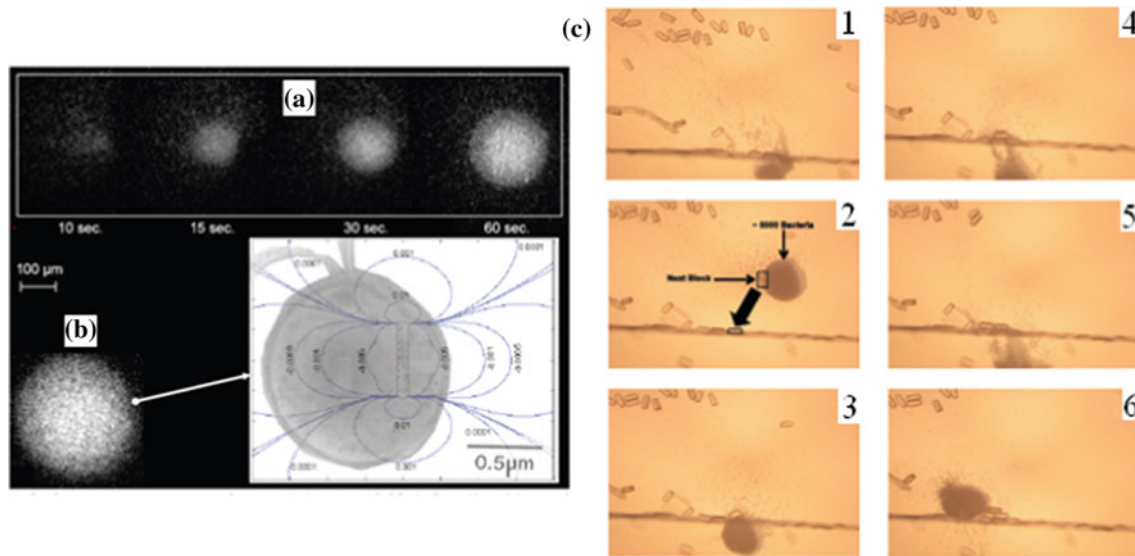


Fig. 22 Swarm or aggregate of several thousand MC-1 flagellated bacteria: **a** example of a formation of a swarm. **b** Image of a larger swarm where *each dot* in the swarm is a MC-1 bacterium shown on the right. The two flagella bundles used for propulsion and the chain

of magnetosomes used for directional control are easily visible on the photograph of the bacterium. **c** Assembly process (Martel and Mohammadi 2010). Reprinted with permission

with some demonstrations of electrical connectivity. However, working assemblies will require more connection types with improved thermal, optical, and structural properties.

- *Part design for assembly* As assembly processes mature and are standardized, designers will need guidelines to help them design parts that will assemble with high accuracy and speed.
- *Process design* In process-directed assembly, the assembly conditions are central to determining the assembly structure, accuracy, and speed. However, models are not currently available to relate most of the process variables to these important assembly process parameters.

The first three areas all relate to the ability to control the assembly process. This will favor the inclusion of active elements and will likely require monitoring and feedback systems. The seeds of potential solutions for many of these challenges have already been demonstrated. Solutions to many of these challenges may be found through the integration of existing concepts. For example, the integration of multiple types of forces in a single process will facilitate orientation control and increased part variety. Additionally, incorporation of active materials such as magnetorheological or thermorheological materials could enable additional control (Krishnan et al. 2009). These systems will also benefit from the incorporation of more closed-loop feedback control systems. It is likely that some advances will come from applying other technologies for microsystem assembly. Some interesting examples include the use of

digital microfluidic systems with droplets as micro-actuators, microfluidic “assembly chambers” (Tolley et al. 2010), and stop-flow lithography (Chung et al. 2008).

8.2 Potential applications

As these processes mature, the application space for these assemblies will increase. Micro/nano-robotics would benefit greatly from these capabilities. Micro-robots utilize small-scale components to create active robotic assemblies. An inexpensive method for integrating smaller components could dramatically decrease the size and/or increase the functionality of the components. Moreover, this technology could significantly contribute to the development of part-directed assembly processes. This type of assembly has recently been proposed through the concept of “smart dust” (Gorder 2003). This concept opens a whole new approach in microscale assembly in which parts could be controlled, and even programmed directly. Although of great complexity, “smart” components would offer significant flexibility for assembly of elaborate structures. When assembly of excessive number of parts is required, manual control of micromanipulator and micro-robots becomes unfeasible due to increased assembly time and effort. Closed-loop control systems, and/or artificial intelligence will be required to identify, grasp and manipulate parts to achieve complex assemblies. Fluid-driven assembly techniques show promising results at positioning components into pre-determined configurations. Similarly, capillary forces are capable of performing assembly

without the need of tool-intervention. While these techniques have been used for many years in SMT alignment, they have the potential to provide the primary alignment means as well in many assembly applications. Fluid-flow control methods, such as the use of microfluidic technology and fluid evaporation, provide a wide variety of positioning strategies (e.g., arrangement into ordered structures and gross positioning within confined spaces). The fast pace of advancements in microfluidics will certainly open more opportunities for adaption to assembly in the future. Additionally, since fluid forces can be applied to components, regardless of functional properties (e.g., magnetic and electric), these fields could form a complementary part of any assembly system that could increase control over the assembly structures.

External field-mediated assembly techniques offers easy and robust control of micro-components in fluidic systems. The low interactions between different fields will enable simultaneous use of these fields in the same application to utilize the advantages of each. For example, orientation control problems may possibly be solved by employing external fields and designing components to respond differently to each field. Magnetic field is most promising for orientation control with its controllable directionality, noninvasive nature and quick response times. The assembly, then, can be accomplished by interactions between individual components or by secondary methods such as solder reflow or evaporation of the liquid.

Biology applications such as tissue engineering and organ printing represent a very challenging assembly problem, but also a very exciting opportunity. These systems typically require fluidic environment to sustain the biological activity of the cells and so fluidic assembly is a natural option. Yet, these tissues have significant complexity in both cell types and structures that must be replicated. Additionally, the cells respond to their environment in complex ways and the environmental conditions that can sustain life are limited. The final performance of the system is sensitive to both the chemical and the mechanical environment in which they reside. While biological growth might be able to achieve complete regeneration under the right circumstances, this is too slow for many applications in regenerative medicine.

Techniques from additive manufacturing could be integrated with fluidic assembly. Layers of different cells could be added sequentially to provide a basic template to facilitate cell growth and effectively reduce regeneration time. Additionally, there is added value for tissues that are made from the patient's own cells. Thus, there is a great opportunity for a system that can programmably assemble components into a functional system that is customized for a particular patient, or even in vivo assembly of those components/cells to eliminate surgery. There is also a great

interest in processes that can bring together the strengths of both organic and inorganic materials to create hybrid systems that function together. Bio-mediated assembly techniques, such as bacteria swarm and DNA-mediated assembly are also becoming more popular with the recent advancements in bioscience. They show great importance for future biological and biomedical assembly applications for bioengineering and tissue engineering, in which non-invasive micro-assembly and manipulation is essential.

SA, digitization and parallel synthesis capabilities of DNA have inspired scientist as a programmable assembly platform. Base-to-base hybridization acting as the binding and driving force to assemble components such as nucleotides, DNA strands or structures (Mastrangeli et al. 2009). Programmability of the DNA-mediated assembly relies on synthetic DNA technology to specifically conjugate sequences with the components attached to them. Electrical connections can be obtained by metallization of DNA's and more complex DNA assemblies can be obtained by patterning of the metalized DNA (Mastrangeli et al. 2009). DNA can further be designed, tailored and assembled to form DNA nano-robots that are capable of mechanical manipulation. The driving force and motion of hybridization between DNA can be employed to manipulate micro- and nanoscale components, attached to DNA. Molecular tweezers capable of opening and closing (Yurke et al. 2000), directional DNA tracks for moving or transporting walker DNA (Shin and Pierce 2004; Yin et al. 2004), and DNA robotic arms (Ding and Seeman 2006) have been reported to date. DNA nano-robots can possibly be utilized in microscale assembly with stronger and controllable interfaces between DNAs and microscale components and for 3D biological assembly on scaffolds for cell cultures and tissues. Bio-mediated assembly techniques also suffer from limitations similar to micro-robotic assembly, as the mechanisms are relatively complex, expensive and not very suitable for assemblies composed of numerous parts. These methods are still at the proof-of-concept level with promising capabilities; however, programmability of the synthetic DNAs is especially very promising for assemblies that require very specific nano- and microscale sequences.

Acknowledgments The authors gratefully acknowledge funding support though the National Science Foundation (NSF CMMI-113075 and CMMI-092637), Sandia National Laboratories, and the Florida Energy Systems Consortium.

References

- Adachi E, Dimitrov AS, Nagayama K (1995) Stripe patterns formed on a glass surface during droplet evaporation. *Langmuir* 11:1057–1060. doi:[10.1021/la00004a003](https://doi.org/10.1021/la00004a003)
- Adams JD, Whitney DE (1999) Application of screw theory to constraint analysis of assemblies of rigid parts. In: *Proceedings*

- of the IEEE International Symposium on Assembly and Task Planning. IEEE, Porto, Portugal, pp 69–74
- Arora WJ, Nichol AJ, Smith HI, Barbastathis G (2006) Membrane folding to achieve three-dimensional nanostructures: nanopatterned silicon nitride folded with stressed chromium hinges. *Appl Phys Lett* 88:1–3
- Arora WJ, Smith HI, Barbastathis G (2007) Membrane folding by ion implantation induced stress to fabricate three-dimensional nanostructures. *Microelectron Eng* 84:1454–1458
- Arcott S, Peytavit E, Vu D et al (2010) Fluidic assembly of hybrid MEMS: a GaAs-based microcantilever spin injector. *J Micro-mech Microeng* 20:025023
- Awatar S, Sevincer E (2006) Elastic averaging in flexure mechanisms: A multi-beam parallelogram flexure case-study. In: 2006 ASME international design engineering technical conferences and computers and information in engineering conference, DETC2006. American Society of Mechanical Engineers, Philadelphia, PA, United States, p 7
- Azam A, Laffin K, Jamal M, Fernandes R (2011) Self-folding micropatterned polymeric containers. *Biomed Microdev* 13:51–58. doi:[10.1007/s10544-010-9470-x](https://doi.org/10.1007/s10544-010-9470-x)
- Bae C, Moon J, Shin H et al (2007) Fabrication of monodisperse asymmetric colloidal clusters by using contact area lithography (CAL). *J Am Chem Soc* 129:14232–14239
- Bahadur V, Garimella SV (2007) Electrowetting-Based Control of Static Droplet States on Rough Surfaces. *Langmuir* 23:4918–4924. doi:[10.1021/la0631365](https://doi.org/10.1021/la0631365)
- Bang Y, Lee K, Kook J et al (2005) Micro parts assembly system with micro gripper and RCC unit. *IEEE Trans Rob* 21:465–470. doi:[10.1109/TRO.2004.838028](https://doi.org/10.1109/TRO.2004.838028)
- Baret J-C, Kleinschmidt F, El Harrak A, Griffiths AD (2009) Kinetic aspects of emulsion stabilization by surfactants: a microfluidic analysis. *Langmuir* 25:6088–6093. doi:[10.1021/la9000472](https://doi.org/10.1021/la9000472)
- Bernassau AL, Ong C-K, Ma Y et al (2011) Two-dimensional manipulation of micro particles by acoustic radiation pressure in a heptagon cell. *IEEE Trans Ultrason Ferroelectr Freq Control* 58:2132–2138. doi:[10.1109/TUFFC.2011.2062](https://doi.org/10.1109/TUFFC.2011.2062)
- Biganzoli F, Fassi I, Pagano C (2005) Development of a gripping system based on capillary force. (ISATP 2005). In: The 6th IEEE international symposium on assembly and task planning: from nano to macro assembly and manufacturing. IEEE, Montreal, Que., Canada, pp 36–40
- Bohringer KF, Srinivasan U, Howe RT (2001) Modeling of capillary forces and binding sites for fluidic self-assembly. In: 14th IEEE international conference on micro electro mechanical systems (MEMS 2001), Jan 21–25 2001. Institute of Electrical and Electronics Engineers Inc, Interlaken, Switzerland, pp 369–374
- Boncheva M, Bruzewicz DA, Whitesides GM (2003) Millimeter-scale self-assembly and its applications. *Pure Appl Chem* 75: 621–630
- Boothroyd G (2005) Assembly automation and product design. Taylor & Francis, Boca Raton, FL
- Boothroyd G, Dewhurst P (1990) Product design decisions anticipate robotic assembly. *Robot World* 8:21–23
- Boothroyd G, Dewhurst P, Knight WA (2002) Product design for manufacture and assembly. Marcel Dekker/Taylor & Francis, New York
- Boreyko JB, Chen C-H (2009) Restoring superhydrophobicity of lotus leaves with vibration-induced dewetting. *Phys Rev Lett* 103:174502
- Bormashenko E, Pogreb R, Whyman G, Erlich M (2007) Resonance Cassie–Wenzel wetting transition for horizontally vibrated drops deposited on a rough surface. *Langmuir* 23:12217–12221. doi:[10.1021/la7016374](https://doi.org/10.1021/la7016374)
- Bos EJC, Bullema JE, Delbressine FLM et al (2008) A lightweight suction gripper for micro assembly. *Precis Eng* 32:100–105. doi:[10.1016/j.precisioneng.2007.05.003](https://doi.org/10.1016/j.precisioneng.2007.05.003)
- Bowden N, Arias F, Deng T, Whitesides GM (2001) Self-assembly of microscale objects at a liquid/liquid interface through lateral capillary forces. *Langmuir* 17:1757–1765
- Boyse JW (1979) Interference detection among solids and surfaces. *Commun ACM* 22:3–9. doi:[10.1145/359046.359048](https://doi.org/10.1145/359046.359048)
- Brakke K (1992) The surface evolver. *Exp Math* 1:141
- Brakke K (2008) The surface evolver. <http://www.susqu.edu/facstaff/b/brakke/evolver/>. Accessed 1 May 2012
- Breen TL (1999) Design and self-assembly of open, regular, 3D mesostructures. *Science* 284:948–951
- Brittain ST, Schueller OJA, Wu H et al (2000) Microorigami: fabrication of small, three-dimensional, metallic structures. *J Phys Chem B* 105:347–350. doi:[10.1021/jp002556e](https://doi.org/10.1021/jp002556e)
- Burgarella S, Merlo S, Dell'Anna B et al (2010) A modular microfluidic platform for cells handling by dielectrophoresis. *Microelectron Eng* 87:2124–2133. doi:[10.1016/j.mee.2010.01.013](https://doi.org/10.1016/j.mee.2010.01.013)
- Burmeister F, Schäfle C, Matthes T et al (1997) Colloid monolayers as versatile lithographic masks. *Langmuir* 13:2983–2987
- Cannon AH, Hua YM, Henderson CL, King WP (2005) Self-assembly for three-dimensional integration of functional electrical components. *J Micromech Microeng* 15:2172–2178
- Cansoy CE, Erbil HY, Akar O, Akin T (2011) Effect of pattern size and geometry on the use of Cassie–Baxter equation for superhydrophobic surfaces. *Colloids Surf A* 386:116–124
- Cappelleri DJ, Cheng P, Fink J et al (2011) Automated assembly for mesoscale parts. *IEEE Trans Autom Sci Eng* 8:598–613. doi:[10.1109/TASE.2011.2132128](https://doi.org/10.1109/TASE.2011.2132128)
- Castellanos A, Ramos A, González A et al (2003) Electrohydrodynamics and dielectrophoresis in microsystems: scaling laws. *J Phys D Appl Phys* 36:2584–2597. doi:[10.1088/0022-3727/36/20/023](https://doi.org/10.1088/0022-3727/36/20/023)
- Cecil J, Vasquez D, Powell D (2005) A review of gripping and manipulation techniques for micro-assembly applications. *Int J Prod Res* 43:819–828
- Chase KW, Greenwood WH (1987) Design issues in mechanical tolerance analysis. In: Advanced topics in manufacturing technology: product design, bioengineering, and space commercialization. Presented at the Winter Annual Meeting of the American Society of Mechanical Engineers. ASME, Boston, MA, USA, pp 11–26
- Chen BK, Zhang Y, Sun Y (2009) Active release of microobjects using a MEMS microgripper to overcome adhesion forces. *J Microelectromech Syst* 18:652–659. doi:[10.1109/JMEMS.2009.2020393](https://doi.org/10.1109/JMEMS.2009.2020393)
- Chen T, Chen L, Sun L et al (2010a) Micro manipulation based on adhesion control with compound vibration BT. In: 23rd IEEE/RSJ 2010 international conference on intelligent robots and systems, IROS 2010, October 18, 2010–October 22, 2010. IEEE Computer Society, Robotics and Microsystems Center, Soochow University, Suzhou 215021, China, pp 6137–6142
- Chen T, Sun L, Chen L et al (2010b) A hybrid-type electrostatically driven microgripper with an integrated vacuum tool. *Sens Actuators A* 158:320–327. doi:[10.1016/j.sna.2010.01.001](https://doi.org/10.1016/j.sna.2010.01.001)
- Chung SE, Park W, Shin S et al (2008) Guided and fluidic self-assembly of microstructures using railed microfluidic channels. *Nat Mater* 7:581–587
- Chung SE, Jung Y, Kwon S (2011) Three-dimensional fluidic self-assembly by axis translation of two-dimensionally fabricated microcomponents in railed microfluidics. *Small (Weinheim an der Bergstrasse, Germany)* 7:796–803
- Clark TD, Ferrigno R, Tien J et al (2002) Template-directed self-assembly of 10- μ m-sized hexagonal plates. *J Am Chem Soc* 124:5419–5426. doi:[10.1021/ja020056o](https://doi.org/10.1021/ja020056o)
- Cohn M (1997) Assembly techniques for microelectromechanical systems. PhD Thesis, University of California, Berkeley

- Conant-Pablos SE, Martinez-Alfaro H, Ikeuchi K (2003) Sensing requirements for robotic assembly from an analysis of critical contact transitions. In: System security and assurance, Oct 5–8 2003. Institute of Electrical and Electronics Engineers Inc, Washington, DC, United States, pp 1834–1839
- Copeland MF, Weibel DB (2009) Bacterial swarming: a model system for studying dynamic self-assembly. *Soft Matter* 5:1174. doi:[10.1039/b812146j](https://doi.org/10.1039/b812146j)
- Crane N, Mishra P, Murray J, Nolas GS (2009) Self-assembly for integration of microscale thermoelectric coolers. *J Electron Mater* 38:1252–1256
- Crane NB, Mishra P, Volinsky AA (2010) Characterization of electrowetting processes through force measurements. *Rev Sci Instrum* 81:43902
- Crane NB, Nelson C, Ni Q, Liberti C (2011) Demonstrations of fluidic manipulation for programmable assembly. Solid Free-form Fabrication Symposium, Austin
- Culpepper ML, Slocum AH, Shaikh FZ, Vrsek G (2004) Quasi-kinematic couplings for low-cost precision alignment of high-volume assemblies. *Trans ASME J Mech Design* 126:456–463
- Dahlmann GW, Yeatman EM, Young PR et al (2001) MEMS high Q microwave inductors using solder surface tension self-assembly. In: Microwave symposium digest, 2001 IEEE MTT-S international, vol 1. Phoenix, AZ, USA, pp 329–332
- Das AN, Zhang P, Lee WH et al (2007) Multiscale, deterministic micro-nano assembly system for construction of on-wafer microrobots. In: 2007 IEEE international conference on robotics and automation, ICRA'07. IEEE, Piscataway, NJ, United States, pp 461–466
- Davies TH (1983a) Mechanical networks—I passivity and redundancy. *Mech Mach Theory* 18:95–112
- Davies TH (1983b) Mechanical networks—II formulae for the degrees of mobility and redundancy. *Mech Mach Theory* 18:103–106
- Davies TH (1983c) Mechanical networks—III Wrenches on circuit screws. *Mech Mach Theory* 18:107–112
- Davies TH (2006) Freedom and constraint in coupling networks. *Proceedings of the Institution of Mechanical Engineers, Part C. J Mech Eng Sci* 220:989–1010. doi:[10.1243/09544062C09105](https://doi.org/10.1243/09544062C09105)
- de Gennes P-G, Quere D, Brochard-Wyart F (2004) Capillarity and wetting phenomena; drops, bubbles, pearls, waves. Springer, New York, p c2004
- Dechev N, Cleghorn W (2002) Micro-assembly of microelectromechanical components into 3-D MEMS. *Canad J Comput Electr Eng* 27:7–15
- Dechev N, Cleghorn WL, Mills JK (2005) Design of grasping interface for microgrippers and micro-parts used in the micro-assembly of MEMS. In: ICIA 2005: 2005 international conference on information acquisition. IEEE, Hong Kong, China, pp 134–139
- Dechev N, Ren L, Liu W et al (2006) Development of a 6 degree of freedom robotic micromanipulator for use in 3D MEMS microassembly. In: 2006 conference on international robotics and automation. IEEE, Orlando, FL, USA, pp 281–288
- Deckman HW, Dunsmuir JH (1982) Natural lithography. *Appl Phys Lett* 41:377. doi:[10.1063/1.93501](https://doi.org/10.1063/1.93501)
- Deegan RD, Bakajin O, Dupont TF et al (1997) Capillary flow as the cause of ring stains from dried liquid drops. *Nature* 389:827–829. doi:[10.1038/39827](https://doi.org/10.1038/39827)
- Deegan R, Bakajin O, Dupont T et al (2000) Contact line deposits in an evaporating drop. *Phys Rev E Stat Phys Plasmas Fluids* 62:756–765
- Dendukuri D, Pregibon DC, Collins J et al (2006) Continuous-flow lithography for high-throughput microparticle synthesis. *Nat Mater* 5:365–369
- Denkov N, Velev O, Kralchevski P et al (1992) Mechanism of formation of two-dimensional crystals from latex particles on substrates. *Langmuir* 8:3183–3190
- Dhindsa MS, Smith NR, Heikenfeld J et al (2006) Reversible electrowetting of vertically aligned superhydrophobic carbon nanofibers. *Langmuir* 22:9030–9034. doi:[10.1021/la061139b](https://doi.org/10.1021/la061139b)
- Di Leonardo R, Ianni F, Ruocco G (2009) Colloidal attraction induced by a temperature gradient. *Langmuir* 25:4247–4250. doi:[10.1021/la8038335](https://doi.org/10.1021/la8038335)
- Diller E, Pawashe C, Floyd S, Sitti M (2011) Assembly and disassembly of magnetic mobile micro-robots towards deterministic 2-D reconfigurable micro-systems. *Int J Robot Res* 30:1667–1680. doi:[10.1177/0278364911416140](https://doi.org/10.1177/0278364911416140)
- Dimitrov AS, Nagayama K (1995) Steady-state unidirectional convective assembling of fine particles into two-dimensional arrays. *Chem Phys Lett* 243:462–468
- Dimitrov AS, Nagayama K (1996) Continuous convective assembling of fine particles into two-dimensional arrays on solid surfaces. *Langmuir* 12:1303–1311
- Dimitrov AS, Miwa T, Nagayama K (1999) A comparison between the optical properties of amorphous and crystalline monolayers of silica particles. *Langmuir* 15:5257–5264
- Ding B, Seeman NC (2006) Operation of a DNA robot arm inserted into a 2D DNA crystalline substrate. *Science (New York, NY)* 314:1583–1585. doi:[10.1126/science.1131372](https://doi.org/10.1126/science.1131372)
- Ding Z, Song W-B, Ziaie B (2009) Sequential droplet manipulation via vibrating ratcheted microchannels. *Sens Actuators B Chem* 142:362–368. doi:[10.1016/j.snb.2009.08.022](https://doi.org/10.1016/j.snb.2009.08.022)
- Dong L, Agarwal AK, Beebe DJ, Jiang HR (2006) Adaptive liquid microlenses activated by stimuli-responsive hydrogels. *Nature* 442:551–554
- Du R, Tang CXY, Zhang DL (2008) Smart devices and machines for advanced manufacturing. In: Wang L, Xi J (eds) Springer, London, pp 367–384
- Edman CF, Swint RB, Gurtner C et al (2000) Electric field directed assembly of an InGaAs LED onto silicon circuitry. *IEEE Photonics Technol Lett* 12:1198–1200. doi:[10.1109/68.874234](https://doi.org/10.1109/68.874234)
- Ellekilde L-P, Petersen HG (2006) Design and test of object aligning grippers for industrial applications. In: 2006 IEEE/RSJ international conference on intelligent robots and systems, IROS. IEEE, Beijing, China, pp 5165–5170
- Elwenspoek M, Abelmann L, Berenschot E et al (2010) Self-assembly of (sub-)micron particles into supermaterials. *J Micromech Microeng* 20:064001
- Enikov ET, Lazarov KV (2001) Optically transparent gripper for microassembly. *Microrobotics and Microassembly III*, October 29, 2001–October 30. SPIE, Newton, MA, USA, pp 40–49
- Erdmann MA, Mason MT (1988) An exploration of sensorless manipulation. *IEEE J Robot Autom* 4:369–379
- Fang JD, Bohringer KF (2006a) Wafer-level packaging based on uniquely orienting self-assembly (The DUO-SPASS processes). *J Microelectromech Syst* 15:531–540
- Fang JD, Bohringer KF (2006b) Wafer-level packaging based on uniquely orienting self-assembly (The DUO-SPASS processes). *J Microelectromech Syst* 15:531–540
- Fazio TD (1987) Generation and consideration of all assembly sequences for assembly system design. In: Proceedings of the 1987 international conference on engineering design—international congress on planning and design theory. ASME, Boston, MA, USA, pp 782–795
- Fearing RS (1995) Survey of sticking effects for micro parts handling. In: International conference on intelligent robots and systems, vol 2. IEEE, Pittsburgh, PA, USA, pp 212–217
- Feddema JT, Xavier P, Brown R (2001) Micro-assembly planning with van der Waals force. *J Micromechatronics* 1:139–153

- Fischer UC (1981) Submicroscopic pattern replication with visible light. *J Vac Sci Technol* 19:881
- Fonstad CG (2002) Magnetically-assisted statistical assembly—a new heterogeneous integration technique. Massachusetts Institute of Technology, Boston, p 6
- Forsberg P, Nikolajeff F, Karlsson M (2011) Cassie–Wenzel and Wenzel–Cassie transitions on immersed superhydrophobic surfaces under hydrostatic pressure. *Soft Matter* 7:104–109
- Fountain TWR, Kailat PV, Abbott JJ (2010) Wireless control of magnetic helical microrobots using a rotating-permanent-magnet manipulator. In: 2010 IEEE international conference on robotics and automation. IEEE, Anchorage, AK, USA, pp 576–581
- Frutiger DR, Vollmers K, Kratochvil BE, Nelson BJ (2009) Small, fast, and under control: wireless resonant magnetic micro-agents. *Int J Robot Res* 29:613–636. doi:[10.1177/0278364909353351](https://doi.org/10.1177/0278364909353351)
- Frutiger DR, Kratochvil BE, Nelson BJ (2010) MagMites - Microrobots for wireless microhandling in dry and wet environments. In: 2010 IEEE international conference on robotics and automation (ICRA), Anchorage, AK, USA, pp 1112–1113
- Furse JE (1981) Kinematic design of fine mechanisms in instruments. *J Phys E Sci Instrum* 14:264–272
- Gao J, Chase KW, Magleby SP (1998) Generalized 3-D tolerance analysis of mechanical assemblies with small kinematic adjustments. *IIE Trans (Institute of Industrial Engineers)* 30:367–377
- Gauthier M, Piat E (2002) An electromagnetic micromanipulation system for single-cell manipulation. *J Micromechatronics* 2:87–119. doi:[10.1163/156856302322756450](https://doi.org/10.1163/156856302322756450)
- Gluskin R (1970) Controlling transport motion with fluidics. *Mech Eng* 92:13–17
- Goemans OC, Goldberg K, van der Stappen AF (2006) Blades: a new class of geometric primitives for feeding 3D parts on vibratory tracks. In: Proceedings 2006 IEEE international conference on robotics and automation, 2006. ICRA 2006. IEEE, Orlando, FL, USA, pp 1730–1736
- Golosovsky M, Saado Y, Davidov D (1999) Self-assembly of floating magnetic particles into ordered structures: a promising route for the fabrication of tunable photonic band gap materials. *Appl Phys Lett* 75:4168. doi:[10.1063/1.125571](https://doi.org/10.1063/1.125571)
- Gorder PF (2003) Sizing up smart dust. *Comput Sci Eng* 5:6–9. doi:[10.1109/MCISE.2003.1238697](https://doi.org/10.1109/MCISE.2003.1238697)
- Gracias DH, Tien J, Breen TL et al (2000) Forming electrical networks in three dimensions by self-assembly. *Science* 289:1170–1172. doi:[10.1126/science.289.5482.1170](https://doi.org/10.1126/science.289.5482.1170)
- Gracias DH, Kavthekar V, Love JC et al (2002) Fabrication of micrometer-scale, patterned polyhedra by self-assembly. *Adv Mater* 14:235–238. doi:[10.1002/1521-4095\(20020205\)14:3<235::AID-ADMA235>3.0.CO;2-B](https://doi.org/10.1002/1521-4095(20020205)14:3<235::AID-ADMA235>3.0.CO;2-B)
- Greiner A, Lienemann J, Korvink JG et al (2002) Capillary forces in micro-fluidic self-assembly. In: 2002 international conference on modeling and simulation of microsystems. Computational Publications, Cambridge, MA 02139, United States, San Juan, Puerto Rico, USA, pp 198–201
- Gro R, Bonani M, Mondada F, Dorigo M (2006) Autonomous self-assembly in swarm-bots. *IEEE Trans Rob* 22:1115–1130. doi:[10.1109/TRO.2006.882919](https://doi.org/10.1109/TRO.2006.882919)
- Gross R, Dorigo M (2008) Self-assembly at the macroscopic scale. *Proc IEEE* 96:1490–1508. doi:[10.1109/JPROC.2008.927352](https://doi.org/10.1109/JPROC.2008.927352)
- Grzybowski BA, Campbell CJ (2004) Complexity and dynamic self-assembly. *Chem Eng Sci* 59:1667–1676. doi:[10.1016/j.ces.2004.01.023](https://doi.org/10.1016/j.ces.2004.01.023)
- Grzybowski BA, Whitesides GM (2001) Macroscopic synthesis of self-assembled dissipative structures. *J Phys Chem B* 105: 8770–8775. doi:[10.1021/jp011187z](https://doi.org/10.1021/jp011187z)
- Grzybowski BA, Whitesides GM (2002) Directed dynamic self-assembly of objects rotating on two parallel fluid interfaces. *J Chem Phys* 116:8571–8577
- Grzybowski BA, Stone HA, Whitesides GM (2000) Dynamic self-assembly of objects rotating at a liquid \pm air interface. *Nature* 405:1033–1036
- Grzybowski BA, Jiang XY, Stone HA, Whitesides GM (2001) Dynamic, self-assembled aggregates of magnetized, millimeter-sized objects rotating at the liquid-air interface: macroscopic, two-dimensional classical artificial atoms and molecules. *Phys Rev E* 6401:11603
- Grzybowski B, Radkowski M, Campbell C (2004) Self-assembling fluidic machines. *Appl Phys Lett* 84:1798–1800
- Gu T, Liu H (2008) The symbolic OBDD scheme for generating mechanical assembly sequences. *Form Methods Syst Design* 33:29–44. doi:[10.1007/s10703-008-0052-y](https://doi.org/10.1007/s10703-008-0052-y)
- Guldiken R, Jo MC, Gallant ND et al (2012) Sheathless size-based acoustic particle separation. *Sensors* 12:905–922. doi:[10.3390/s120100905](https://doi.org/10.3390/s120100905)
- Guo X, Li H, Ahn BY et al (2009) Two- and three-dimensional folding of thin film single-crystalline silicon for photovoltaic power applications. *Proc Nat Acad Sci USA* 106:20149–20154. doi:[10.1073/pnas.0907390106](https://doi.org/10.1073/pnas.0907390106)
- Hale LC, Slocum AH (2001) Optimal design techniques for kinematic couplings. *Precis Eng* 25:114–127
- Harsh K, Lee YC (1998) Modeling for solder self-assembled MEMS. Micro-optics integration and assemblies. SPIE-International Society Optical Engineering, San Jose, pp 177–184
- Harsh K, Bright V, Lee Y (1999a) Solder self-assembly for three-dimensional microelectromechanical systems. *Sens Actuators A* 77:237–244
- Harsh KF, Bright VM, Lee YC (1999b) Solder self-assembly for three-dimensional microelectromechanical systems. *Sens Actuators A* 77:237–244
- Hayashi T (1992) An innovative bonding technique for optical chips using solder bumps that eliminate chip positioning adjustments. *IEEE Trans Compon Hybrids Manuf Technol* 15:225–230. doi:[10.1109/33.142898](https://doi.org/10.1109/33.142898)
- Hosokawa K, Shimoyama I, Miura H (1994) Dynamics of self-assembling systems—analogy with chemical kinetics. In: Proceedings of the fourth international workshop on the syntheses and simulation of living systems. MIT Press, Cambridge, MA, USA, pp 172–180
- Hu H, Larson RG (2006) Marangoni effect reverses coffee-ring depositions. *J Phys Chem B* 110:7090–7094. doi:[10.1021/jp0609232](https://doi.org/10.1021/jp0609232)
- Hu W, Ishii KS, Ohta AT (2011) Micro-assembly using optically controlled bubble microrobots. *Appl Phys Lett* 99:94103
- Huang J, Kim F, Tao AR et al (2005) Spontaneous formation of nanoparticle stripe patterns through dewetting. *Nat Mater* 4: 896–900
- Huck WTS, Tien J, Whitesides GM (1998) Three-dimensional mesoscale self-assembly. *J Am Chem Soc* 120:8267–8268
- Hughes MP (2000) AC electrokinetics: applications for nanotechnology. *Nanotechnology* 11:124–132. doi:[10.1088/0957-4484/11/2/314](https://doi.org/10.1088/0957-4484/11/2/314)
- Hulteen JC, Van Duyne RP (1995) Nanosphere lithography: a materials general fabrication process for periodic particle array surfaces. *J Vac Sci Technol A Vac Surf Films* 13:1553. doi:[10.1116/1.579726](https://doi.org/10.1116/1.579726)
- Jacobs HO, Tao AR, Schwartz A et al (2002) Fabrication of a cylindrical display by patterned assembly. *Science* 296:323–325
- Jamal M, Bassik N, Cho J-H et al (2010) Directed growth of fibroblasts into three dimensional micropatterned geometries via self-assembling scaffolds. *Biomaterials* 31:1683–1690
- Janjua M, Nudurupati S, Singh P, Aubry N (2011) Electric field-induced self-assembly of micro- and nanoparticles of various shapes at two-fluid interfaces. *Electrophoresis* 32:518–526. doi:[10.1002/elps.201000523](https://doi.org/10.1002/elps.201000523)

- Jayaram U, Kim Y, Jayaram S et al (2004) Reorganizing CAD assembly models (as-designed) for manufacturing Simulations and planning (as-built). *Trans ASME J Comput Inf Sci Eng* 4:98–108. doi:[10.1115/1.1737772](https://doi.org/10.1115/1.1737772)
- Jeong JS, Lee JW, Lee CY et al (2011) Particle manipulation in a microfluidic channel using acoustic trap. *Biomed Microdevices* 13:779–788. doi:[10.1007/s10544-011-9548-0](https://doi.org/10.1007/s10544-011-9548-0)
- Jia K, Yang K, Fan Z, Ju B-F (2012) A contactless methodology of picking up micro-particles from rigid surfaces by acoustic radiation force. *Rev Sci Instrum* 83:014902. doi:[10.1063/1.3676636](https://doi.org/10.1063/1.3676636)
- Jiang L, Erickson D (2011) Directed self-assembly of microcomponents enabled by laser-activated bubble latching. *Langmuir* 27:11259–11264. doi:[10.1021/la2019617](https://doi.org/10.1021/la2019617)
- Jones TB (2005) An electromechanical interpretation of electrowetting. *J Micromech Microeng* 15:1184
- Jones TB, Kraybill JP (1986) Active feedback-controlled dielectrophoretic levitation. *J Appl Phys* 60:1247. doi:[10.1063/1.337345](https://doi.org/10.1063/1.337345)
- Joshi AS, Sun Y (2010) Numerical simulation of colloidal drop deposition dynamics on patterned substrates for printable electronics fabrication. *J Display Technol* 6:579–585. doi:[10.1109/JDT.2010.2040707](https://doi.org/10.1109/JDT.2010.2040707)
- Kaler KVIS, Tai AKC (1988) Dynamic (active feedback controlled) dielectrophoretic levitation of Canola protoplasts. In: *Proceedings of the annual international conference of the IEEE engineering in medicine and biology society*, vol 1. IEEE, New Orleans, LA, USA, pp 267–268
- Kalontarov M, Tolley MT, Lipson H, Erickson D (2010) Hydrodynamically driven docking of blocks for 3D fluidic assembly. *Microfluid Nanofluid* 9:551–558. doi:[10.1007/s10404-010-0572-0039](https://doi.org/10.1007/s10404-010-0572-0039)
- Kasaya T, Miyazaki H, Saito S, Sato T (1999) Micro object handling under SEM by vision-based automatic control. In: *Proceedings of international conference on robotics and automation*. IEEE, Piscataway, NJ, USA, pp 2189–2196
- Katz E, Yarin AL, Salalha W, Zussman E (2006) Alignment and self-assembly of elongated micron size rods in several flow fields. *J Appl Phys* 100:34312–34313
- Kim D-H, Kim B, Kang H (2004) Development of a piezoelectric polymer-based sensorized microgripper for microassembly and micromanipulation. *Microsyst Technol* 10:275–280. doi:[10.1007/s00542-003-0330-y](https://doi.org/10.1007/s00542-003-0330-y)
- Kim J-H, Liu G, Kim SH (2006) Deposition of stable hydrophobic coatings with in-line CH₄ atmospheric rf plasma. *J Mater Chem* 16:977–981
- Kim SH, Hashi S, Ishiyama K (2011) Magnetic actuation based snake-like mechanism and locomotion driven by rotating magnetic field. *IEEE Trans Magn* 47:3244–3247. doi:[10.1109/TMAG.2011.2143698](https://doi.org/10.1109/TMAG.2011.2143698)
- Klavins E, Ghrist R, Lipsky D (2006) A grammatical approach to self-organizing robotic systems. *IEEE Trans Autom Control* 51:949–962
- Knuesel RJ, Jacobs HO (2010) Self-assembly of microscopic chiplets at a liquid–liquid–solid interface forming a flexible segmented monocrystalline solar cell. *Proc Nat Acad Sci USA* 107:993–998
- Knuesel RJ, Park S, Zheng W, Jacobs HO (2012) Self-assembly and self-tiling: integrating active dies across length scales on flexible substrates. *J Microelectromech Syst* 21:85–99
- Koishi T, Yasuoka K, Fujikawa S et al (2009) Coexistence and transition between Cassie and Wenzel state on pillared hydrophobic surface. *Proc Nat Acad Sci* 106:8435–8440
- Kralchevsky PA, Nagayama K (2001) *Particles at fluids interfaces and membranes: attachment of colloid particles and proteins to interfaces and formation of two-dimensional arrays*/Peter A. Kralchevsky, Kuniaki Nagayama. Elsevier, Amsterdam, New York
- Krishnamoorthy AV, Goossen KW (1998) Optoelectronic-VLSI: photonics integrated with VLSI circuits. *IEEE J Sel Top Quantum Electron* 4:899–912. doi:[10.1109/2944.736073](https://doi.org/10.1109/2944.736073)
- Krishnan M, Tolley MT, Lipson H, Erickson D (2008) Increased robustness for fluidic self-assembly. *Phys Fluids* 20:73304
- Krishnan M, Tolley MT, Lipson H, Erickson D (2009) Hydrodynamically tunable affinities for fluidic assembly. *Langmuir* 25:3769–3774. doi:[10.1021/la803517f](https://doi.org/10.1021/la803517f)
- Krupenkin TN, Taylor JA, Wang EN et al (2007) Reversible wetting–dewetting transitions on electrically tunable superhydrophobic nanostructured surfaces. *Langmuir* 23:9128–9133. doi:[10.1021/la7008557](https://doi.org/10.1021/la7008557)
- Kumar A, Whitesides GM (1993) Features of gold having micrometer to centimeter dimensions can be formed through a combination of stamping with an elastomeric stamp and an alkanethiol “ink” followed by chemical etching. *Appl Phys Lett* 63:2002–2004
- Kumar S, Seo Y-K, Kim G-H (2009) Manipulation and trapping of semiconducting ZnO nanoparticles into nanogap electrodes by dielectrophoresis technique. *Appl Phys Lett* 94:153104. doi:[10.1063/1.3118588](https://doi.org/10.1063/1.3118588)
- Kwon JO, Yang JS, Chung SK (2011) Untethered microrobot actuated by an electromagnetic field with an acoustically oscillating bubble for bio/micro-object manipulation. In: *16th international solid-state sensors, actuators and microsystems conference (TRANSDUCERS)*, 2011. IEEE, Beijing, China, pp 282–285
- Lambert P, Delchambre A (2005) Design rules for a capillary gripper in microassembly (ISATP 2005). In: *The 6th IEEE international symposium on assembly and task planning: from nano to macro assembly and manufacturing*. IEEE, Montreal, Quebec, Canada, pp 67–73
- Lanham J, Dialami F (2001) The assembly state vector: a new approach to the generation of assembly sequences. In: *Proceedings of the 2001 IEEE international symposium on assembly and task planning (ISATP2001)* assembly and disassembly in the twenty-first century. IEEE, Fukuoka, Japan, pp 37–42
- Lappa M (2010) *Thermal Convection [electronic resource]: patterns, evolution and stability*. Wiley, Hoboken
- Lee SW, Bashir R (2003) Dielectrophoresis and electrohydrodynamics-mediated fluidic assembly of silicon resistors. *Appl Phys Lett* 83:3833. doi:[10.1063/1.1624642](https://doi.org/10.1063/1.1624642)
- Lee SW, Bashir R (2005) Dielectrophoresis and chemically mediated directed self-assembly of micrometer-scale three-terminal metal oxide semiconductor field-effect transistors. *Adv Mater* 17:2671–2677. doi:[10.1002/adma.200501048](https://doi.org/10.1002/adma.200501048)
- Lee J, Lee C, Shung KK (2010a) Calibration of sound forces in acoustic traps. *IEEE Trans Ultrason Ferroelectr Freq Control* 57:2305–2310. doi:[10.1109/TUFFC.2010.1691](https://doi.org/10.1109/TUFFC.2010.1691)
- Lee J, Teh S-Y, Lee A et al (2010b) Transverse acoustic trapping using a gaussian focused ultrasound. *Ultrasound Med Biol* 36:350–355. doi:[10.1016/j.ultrasmedbio.2009.10.005](https://doi.org/10.1016/j.ultrasmedbio.2009.10.005)
- Leong TG, Lester PA, Koh TL et al (2007) Surface tension-driven self-folding polyhedra. *Langmuir* 23:8747–8751
- Leong TG, Zarafshar AM, Gracias DH (2010) Three-dimensional fabrication at small size scales. *Small* 6:792–806
- Linderman RJ, Kladitis PE, Bright VM (2002) Development of the micro rotary fan. *Sens Actuators A* 95:135–142
- Liu C, Qiao H, Zhang B (2011a) Stable sensorless localization of 3-D objects. *IEEE Trans Syst Man Cybern Part C (Appl Rev)* 41:923–941. doi:[10.1109/TSMCC.2011.2109948](https://doi.org/10.1109/TSMCC.2011.2109948)
- Liu G, Fu L, Rode AV, Craig VSJ (2011b) Water droplet motion control on superhydrophobic surfaces: exploiting the Wenzel-to-Cassie transition. *Langmuir* 27:2595–2600. doi:[10.1021/la104669k](https://doi.org/10.1021/la104669k)

- Lopez-Walle B, Gauthier M, Chaillet N (2008) Principle of a submerged freeze gripper for microassembly. *IEEE Trans Rob* 24:897–902. doi:[10.1109/TRO.2008.924944](https://doi.org/10.1109/TRO.2008.924944)
- Love JC, Urbach AR, Prentiss MG, Whitesides GM (2003) Three-dimensional self-assembly of metallic rods with submicron diameters using magnetic interactions. *J Am Chem Soc* 125:12696–12697. doi:[10.1021/ja037642h](https://doi.org/10.1021/ja037642h)
- Lu H, Bailey C (2005) Dynamic analysis of flip-chip self-alignment. *IEEE Trans Adv Packag* 28:475–480
- Maenosono S, Dushkin CD, Saita S, Yamaguchi Y (1999) Growth of a semiconductor nanoparticle ring during the drying of a suspension droplet. *Langmuir* 15:957–965
- Mantripragada R, Whitney DE (1998) The datum flow chain: a systematic approach to assembly design and modeling. *Res Eng Design* 10:150–165
- Manukyan G, Oh JM, van den Ende D et al (2011) Electrical switching of wetting states on superhydrophobic surfaces: a route towards reversible Cassie-to-Wenzel transitions. *Phys Rev Lett* 106:14501
- Marentis TC, Vacanti JP, Hsiao JC, Borenstein JT (2009) Elastic averaging for assembly of three-dimensional constructs from elastomeric micromolded layers. *J Microelectromech Syst* 18:531–538. doi:[10.1109/JMEMS.2009.2018372](https://doi.org/10.1109/JMEMS.2009.2018372)
- Martel S (2005) Method and system for controlling micro-objects or micro-particles. US Patent US 2006/0073540 A1
- Martel S (2006) Controlled Bacterial Micro-actuation. In: 2006 international conference on microtechnologies in medicine and biology. IEEE, Okinawa, Japan, pp 89–92
- Martel S, Mohammadi M (2010) Using a swarm of self-propelled natural microrobots in the form of flagellated bacteria to perform complex micro-assembly tasks. In: 2010 IEEE international conference on robotics and automation. IEEE, Anchorage, AK, USA, pp 500–505
- Mastrangeli M, Abbasi S, Varel C et al (2009) Self-assembly from milli- to nanoscales: methods and applications. *J Micromech Microeng Struct Dev Syst* 19:83001. doi:[10.1088/0960-1317/19/8/083001](https://doi.org/10.1088/0960-1317/19/8/083001)
- Matsushita SI, Yagi Y, Miwa T et al (2000) Light propagation in composite two-dimensional arrays of polystyrene spherical particles. *Langmuir* 16:636–642
- Meitinger T, Pfeiffer F (1994) Automated assembly with compliant mating parts. In: Proceedings of the 1994 IEEE international conference on robotics and automation. IEEE, San Diego, CA, USA, pp 1462–1467
- Meitinger T, Pfeiffer F (1997) Modelling and simulation of assembly processes with robots. *Appl Math Comput Sci* 7:343–375
- Menciassi A, Eisinger A, Izzo I, Dario P (2004) From “macro” to “micro” manipulation: models and experiments. *Mechatronics IEEE/ASME Trans Mechatronics* 9:311–320
- Moll M, Goldberg K, Erdmann MA, Fearing R (2002) Orienting micro-scale parts with squeeze and roll primitives. In: Robotics and automation, 2002. Proceedings. IEEE international conference on ICRA’02, vol 2. Washington, DC, USA, pp 1931–1936
- Moon I, Kim J (2006) Using EWOD (electrowetting-on-dielectric) actuation in a micro conveyor system. *Sens Actuators A* 130–131:537–544
- Morris CJ, Parviz BA (2006) Self-assembly and characterization of Marangoni microfluidic actuators. *J Micromech Microeng* 16:972–980
- Morris CJ, Parviz BA (2008) Micro-scale metal contacts for capillary force-driven self-assembly. *J Micromech Microeng* 18:015022. doi:[10.1088/0960-1317/18/1/015022](https://doi.org/10.1088/0960-1317/18/1/015022)
- Morris CJ, Stauth SA, Parviz BA (2005) Self-assembly for microscale and nanoscale packaging: steps toward self-packaging. *IEEE Trans Adv Packag* 28:600–611
- Mugele F, Baret JC (2005) Electrowetting: from basics to applications. *J Phys Condens Matter* 17:R705
- Myers D (1991) Surfaces, interfaces, and colloids: principles and applications. VCH Publishers, New York
- Napp N, Burden S, Klavins E (2006) The statistical dynamics of programmed self-assembly. In: 2006 IEEE international conference on robotics and automation, ICRA 2006. IEEE, Orlando, FL, United States, pp 1469–1476
- Nasiatka PJ, Karim ZS (1995) Determination of optimal solder volume for precision self-alignment of BGA using flip-chip bonding. In: Proceedings of electron devices meeting, 1995, 1995 IEEE Hong Kong, pp 6–9
- Nelson WC, Kim C-J (2012) Droplet actuation by electrowetting-on-dielectric (EWOD): a review. *J Adhes Sci Technol* 26:1747–1771. doi:[10.1163/156856111X599562](https://doi.org/10.1163/156856111X599562)
- Nelson CW, Lynch CM, Crane NB (2011) Continuous electrowetting via electrochemical diodes. *Lab Chip* 11:2149–2152
- Neubert J, Cantwell AP, Constantin S et al (2010) A robotic module for stochastic fluidic assembly of 3D self-reconfiguring structures. In: 2010 IEEE international conference on robotics and automation. IEEE, pp 2479–2484
- Ng JMK, Fuerstman MJ, Grzybowski BA et al (2003) Self-assembly of gears at a fluid/air interface. *J Am Chem Soc* 125:7948–7958. doi:[10.1021/ja0347235](https://doi.org/10.1021/ja0347235)
- Ni Q, Crane NB, Guldiken RO (2011) Ultrasonic excitation induced Wenzel to Cassie transition. In: Proceedings of the ASME 2011 international mechanical engineering congress and exposition. Denver, CO, USA, pp 11–13
- Nichol AJ, Stellman PS, Arora WJ, Barbastathis G (2007) Two-step magnetic self-alignment of folded membranes for 3D nanomanufacturing. *Microelectron Eng* 84:1168–1171
- O’Kane JM, LaValle SM (2005) Almost-sensorless localization BT—2005 IEEE international conference on robotics and automation, April 18, 2005–April 22, 2005. Institute of Electrical and Electronics Engineers Inc., Barcelona, pp 3764–3769
- O’Riordan A, Delaney P, Redmond G (2004) Field configured assembly: programmed manipulation and self-assembly at the mesoscale. *Nano Lett* 4:761–765. doi:[10.1021/nl034145q](https://doi.org/10.1021/nl034145q)
- Ohasi T, Iwata M, Arimoto S, Miyakawa S (2002) Extended assemblability evaluation method (AEM): (extended quantitative assembly producibility evaluation for assembled parts and products). *JSME Int J Ser C* 45:567–574
- Oliver SRJ, Clark TD, Bowden N, Whitesides GM (2001) Three-dimensional self-assembly of complex, millimeter-scale structures through capillary bonding. *J Am Chem Soc* 123:8119–8120
- Ozdemir T, Sandal D, Culha M et al (2010) Assembly of magnetic nanoparticles into higher structures on patterned magnetic beads under the influence of magnetic field. *Nanotechnology* 21:125603. doi:[10.1088/0957-4484/21/12/125603](https://doi.org/10.1088/0957-4484/21/12/125603)
- Park J, Moon J (2006) Control of colloidal particle deposit patterns within picoliter droplets ejected by ink-jet printing. *Langmuir ACS J Surf Colloids* 22:3506–3513. doi:[10.1021/la053450j](https://doi.org/10.1021/la053450j)
- Park SH, Xia Y (1999) Assembly of mesoscale particles over large areas and its application in fabricating tunable optical filters. *Langmuir* 15:266–273
- Park W, Lee HS, Park H, Kwon S (2009) Sorting microparticles by orientation using wedged-fin and railed microfluidics. In: TRANSDUCERS 2009–2009 international solid-state sensors, actuators and microsystems conference. IEEE, Denver, CO, United States, pp 429–432
- Park KS, Xiong X, Baskaran R, Bohringer KF (2011) Part scaling and mechanics of thin part self-assembly in the fluidic phase. In: 2011 IEEE 24th international conference on micro electro mechanical systems. IEEE, Cancun, Mexico, pp 364–367

- Pawashe C, Floyd S, Sitti M (2009) Modeling and experimental characterization of an untethered magnetic micro-robot. *Int J Robot Res* 28:1077–1094. doi:[10.1177/0278364909341413](https://doi.org/10.1177/0278364909341413)
- Pelesko JA (2007) Self assembly: the science of things that put themselves together, (2006). Chapman and Hall/CRC, Boca Raton 336
- Perkins JM (2002) Magnetically assisted statistical assembly of III–V heterostructures on silicon. Massachusetts Institute of Technology, Cambridge, MA, p 75
- Pethig R (1979) Dielectric and electronic properties of biological materials. Wiley, Chichester, NY, p 376
- Pieranski P, Strzelecki L, Pansu B (1983) Thin colloidal crystals. *Phys Rev Lett* 50:900–903
- Pohl HA (1951) The motion and precipitation of suspensions in divergent electric fields. *J Appl Phys* 22:869–871
- Popa DO, Lee WH, Murthy R et al (2007) High yield automated MEMS assembly. In: 3rd IEEE international conference on automation science and engineering. IEEE, Scottsdale, AZ, USA, pp 1099–1104
- Potsaid B, Bellouard Y, Wen JT (2005) Adaptive scanning optical microscope (ASOM): a multidisciplinary optical microscope design for large field of view and high resolution imaging. *Opt Express* 13:6504–6518. doi:[10.1364/OPEX.13.006504](https://doi.org/10.1364/OPEX.13.006504)
- Potsaid B, Wen JT, Bellouard Y (2006) Adaptive scanning optical microscope (ASOM) for large workspace micro-robotic applications. In: Proceedings 2006 IEEE international conference on robotics and automation, 2006. ICRA 2006. IEEE, Orlando, FL, USA, pp 1024–1029
- Puttlitz KJ, Totta P (2001) Area array interconnection handbook. Kluwer Academic Publishers, Boston
- Py C, Reverdy P, Doppler L et al (2007) Capillary origami: spontaneous wrapping of a droplet with an elastic sheet. *Phys Rev Lett* 98:156103
- Ramados V, Crane NB (2008) Design of fluidic self-assembly bonds for precise component positioning. Photonics packaging, integration, and interconnects VIII. SPIE, San Jose, p 68990
- Randall CL, Gultepe E, Gracias DH (2012) Self-folding devices and materials for biomedical applications. *Trends Biotechnol* 30: 138–146
- Roach LS, Song H, Ismagilov RF (2004) Controlling nonspecific protein adsorption in a Pplug-based microfluidic system by controlling interfacial chemistry using fluorosurfactants. *Anal Chem* 77:785–796. doi:[10.1021/ac049061w](https://doi.org/10.1021/ac049061w)
- Rogers JA, Nuzzo RG (2005) Recent progress in soft lithography. *Mater Today* 8:50–56
- Rudenko OV, Lebedev-Stepanov PV, Gusev VA et al (2010) Control of the self-assembly processes in a droplet of a colloidal solution by an acoustic field. *Acoust Phys* 56:935–941. doi:[10.1134/S1063771010060187](https://doi.org/10.1134/S1063771010060187)
- Salalha W, Zussman E (2005) Investigation of fluidic assembly of nanowires using a droplet inside microchannels. *Phys Fluids* 17:063301. doi:[10.1063/1.1925047](https://doi.org/10.1063/1.1925047)
- Schneider TM, Mandre S, Brenner MP (2011) Algorithm for a microfluidic assembly line. *Phys Rev Lett* 106:094503. doi:[10.1103/PhysRevLett.106.094503](https://doi.org/10.1103/PhysRevLett.106.094503)
- Schouten CH, Rosielle PCJN, Schellekens PHJ (1997) Design of a kinematic coupling for precision applications. *Precis Eng* 20: 46–52
- Seth A, Vance JM, Oliver JH (2010) Combining dynamic modeling with geometric constraint management to support low clearance virtual manual assembly. *J Mech Design* 132:081002. doi:[10.1115/1.4001565](https://doi.org/10.1115/1.4001565)
- Shastri A, Taylor D, Bohringer KF (2007) Micro-structured surface ratchets for droplet transport. In: International solid-state sensors, actuators and microsystems conference, 2007. TRANSDUCERS 2007. Lyon, France, pp 1353–1356
- Shet S, Mehta VR, Fiory AT et al (2004) The magnetic field-assisted assembly of nanoscale semiconductor devices: a new technique. *JOM* 56:32–34
- Shetye SB, Agashe JS, Arnold DP (2007) Investigation of microscale magnetic forces for magnet array self-assembly. *IEEE Trans Magn* 43:2713–2715
- Shetye SB, Eskinazi I, Arnold DP (2009) Part-to-part and part-to-substrate magnetic self-assembly of millimeter scale components with angular orientation. In: 2009 IEEE 22nd international conference on micro electro mechanical systems. IEEE, Sorrento, Italy, pp 669–672
- Shin J-S, Pierce NA (2004) A synthetic DNA walker for molecular transport. *J Am Chem Soc* 126:10834–10835. doi:[10.1021/ja047543j](https://doi.org/10.1021/ja047543j)
- Shukla G, Whitney DE (2001) Systematic evaluation of constraint properties of datum flow chain. In: 2001 IEEE international symposium on assembly and task planning (ISATP2001), May 28–29 2001. Fukuoka, pp 337–343
- Shukla G, Whitney DE (2005) The path method for analyzing mobility and constraint of mechanisms and assemblies. *IEEE Trans Autom Sci Eng* 2:184–192
- Singh BP, Onozawa K, Yamanaka K et al (2005) Novel high precision optoelectronic device fabrication technique using guided fluidic assembly. *Opt Rev* 12:345–351
- Slocum AH (1988) Kinematic couplings for precision fixturing part 1: formulation of design parameters. *Precis Eng* 10:85–91
- Slocum AH (1992) Precision machine design. Society of Manufacturing Engineers, Dearborn 750
- Slocum AH, Donmez A (1988) Kinematic couplings for precision fixturing—part 2: experimental determination of repeatability and stiffness. *Precis Eng* 10:115–122
- Slocum AH, Weber AC (2003) Precision passive mechanical alignment of wafers. *J Microelectromech Syst* 12:826–834
- Soga I, Ohno Y, Kishimoto S et al (2003) Fluidic assembly of thin GaAs blocks on Si substrates. *Jpn J Appl Phys* 42:2226–2229
- Solovev AA, Sanchez S, Pumera M et al (2010) Magnetic control of tubular catalytic microbots for the transport, assembly, and delivery of micro-objects. *Adv Funct Mater* 20:2430–2435. doi:[10.1002/adfm.200902376](https://doi.org/10.1002/adfm.200902376)
- Springer GH, Higgins DA (2000) Multiphoton-excited fluorescence imaging and photochemical modification of dye-doped polystyrene microsphere arrays. *Chem Mater* 12:1372–1377
- Sprumont F, Muller J-P (1997) AMACIOA: a multiagent system for designing flexible assembly lines. In: First international conference on practical application of intelligent agents and multi-agent technology (PAAM). Taylor & Francis, London, UK, pp 573–589
- Srinivasan U, Liepmann D, Howe RT (2001) Microstructure to substrate self-assembly using capillary forces. *J Microelectromech Syst* 10:17–24. doi:[10.1109/84.911087](https://doi.org/10.1109/84.911087)
- Stauth SA, Parviz BA (2006) Self-assembled single-crystal silicon circuits on plastic. *Proc Nat Acad Sci USA* 103:13922–13927
- Steager E, Kim C-B, Patel J et al (2007) Control of microfabricated structures powered by flagellated bacteria using phototaxis. *Appl Phys Lett* 90:263901. doi:[10.1063/1.2752721](https://doi.org/10.1063/1.2752721)
- Sun S (2000) Monodisperse FePt Nanoparticles and Ferromagnetic FePt Nanocrystal Superlattices. *Science* 287:1989–1992
- Sun C, Zhao X-W, Han Y-H, Gu Z-Z (2008) Control of water droplet motion by alteration of roughness gradient on silicon wafer by laser surface treatment. *Thin Solid Films* 516:4059–4063
- Syms RRA (1999) Surface tension powered self-assembly of 3-D micro-optomechanical structures. *J Microelectromech Syst* 8:448–455. doi:[10.1109/84.809060](https://doi.org/10.1109/84.809060)
- Syms RRA, Yeatman EM (1993) Self-assembly of three-dimensional microstructures using rotation by surface tension forces. *Electron Lett* 29:662

- Syms RA, Yeatman E, Brigh VM, Whitesides GM (2003) Surface tension-powered self-assembly of microstructures-the state-of-the-art. *J Microelectromech Syst* 12:387–417
- Tolley MT, Krishnan M, Erickson D, Lipsen H (2008) Dynamically programmable fluidic assembly. *Appl Phys Lett* 93:254105
- Tolley MT, Kalontarov M, Neubert J et al (2010) Stochastic modular robotic systems: a study of fluidic assembly strategies. *IEEE Trans Rob* 26:518–530. doi:[10.1109/TRO.2010.2047299](https://doi.org/10.1109/TRO.2010.2047299)
- Tottori S, Sugita N, Kometani R et al (2011) Selective control method for multiple magnetic helical microrobots. *J Micro Nano Mechatron* 6:1–7. doi:[10.1007/s12213-011-0035-8](https://doi.org/10.1007/s12213-011-0035-8)
- Udeshi T, Tsui K (2005) Assembly sequence planning for automated micro assembly. In: 2005 IEEE international symposium on assembly and task planning (ISATP). IEEE, Zyvx Corp., Richardson, TX, USA, pp 98–105
- Vanapalli SA, Iacovella CR, Sung KE et al (2008) Fluidic assembly and packing of microspheres in confined channels. *Langmuir ACS J Surf Colloids* 24:3661–3670
- Vasudev A, Zhe J (2008) A capillary microgripper based on electrowetting. *Appl Phys Lett* 93:103503. doi:[10.1063/1.2978402](https://doi.org/10.1063/1.2978402)
- Vasudev A, Jagtiani A, Du L, Zhe J (2009) A low-voltage droplet microgripper for micro-object manipulation. *J Micromech Microeng* 19:075005
- Velev OD, Kaler EW (2000) Structured porous materials via colloidal crystal templating: from inorganic oxides to metals. *Adv Mater* 12:531–534
- Velev OD, Lenhoff AM (2000) Colloidal crystals as templates for porous materials. *Curr Opin Colloid Interface Sci* 5:56–63
- Verheijen HJJ, Prins MWJ (1999) Contact angles and wetting velocity measured electrically. *Rev Sci Instrum* 70:3668–3673
- Verma AK, Hadley MA, Yeh H-JJ, Smith JS (1995) Fluidic self-assembly of silicon microstructures. In: Proceedings of 45th electronic components and technology conference, 1995. IEEE, Las Vegas, NV, USA, pp 1263–1268
- Vidvasagar A, Majewski J, Toomey R (2008) Temperature induced volume-phase transitions in surface-tethered poly(N-isopropylacrylamide) networks. *Macromolecules* 41:919–924
- Vollmers K, Frutiger DR, Kratochvil BE, Nelson BJ (2008) Wireless resonant magnetic microactuator for untethered mobile microrobots. *Appl Phys Lett* 92:144103. doi:[10.1063/1.2907697](https://doi.org/10.1063/1.2907697)
- Wale MJ, Edge C (1990) Self-aligned flip-chip assembly of protonic devices with electrical and optical connections. *IEEE Trans Compon Hybrids Manuf Technol* 13:780–786. doi:[10.1109/33.62593](https://doi.org/10.1109/33.62593)
- Watanabe S, Inukai K, Mizuta S, Miyahara MT (2009) Mechanism for stripe pattern formation on hydrophilic surfaces by using convective self-assembly. *Langmuir ACS J Surf Colloids* 25:7287–7295
- Wei H, Chen Y, Liu M et al (2011) Swarm robots: from self-assembly to locomotion. *Comput J* 54:1465–1474. doi:[10.1093/comjnl/bxq072](https://doi.org/10.1093/comjnl/bxq072)
- Whitesides GM, Grzybowski B (2002) Self-assembly at all scales. *Science* 295:2418–2421
- Whitney DE (1982) Quasi-static assembly of compliantly supported rigid parts. *J Dyn Syst Measure Control Trans ASME* 104:65–77
- Whitney DE (1987) Historical perspective and state of the art in robot force feedback. *Int J Robot Res* 6:3–14
- Whitney DE (2004) Mechanical assemblies: their design, manufacture, and role in product development, 1st edn. Oxford University Press, New York, NY, p 517
- Whitney DE, Nevins JL (1982) What is the remote center compliance (RCC) and what can I do? In: Robotics today. Robotics international, society of manufacturing engineers, pp 3–15
- Whitney DE, Gustavson RE, DeFazio TL et al (1983) Part mating theories for compliant parts. In: 10th Conference on production research and technology. SAE, Warrendale, PA, USA, Detroit, MI, Engl, pp 111–117
- Whitney DE, Gilbert OL, Jastrzebski M (1994) Representation of geometric variations using matrix transforms for statistical tolerance analysis in assemblies. *Res Eng Design* 6:191–210
- Wolfe DB, Snead A, Mao C et al (2003) Mesoscale self-assembly: capillary interactions when positive and negative menisci have similar amplitudes. *Langmuir* 19:2206–2214
- Wu HK, Bowden N, Whitesides GM (1999) Selectivities among capillary bonds in mesoscale self-assembly. *Appl Phys Lett* 75:3222–3224
- Xia Y, Gates B, Yin Y, Lu Y (2000) Monodispersed colloidal spheres: old materials with new applications. *Adv Mater* 12:693–713
- Xia D, Biswas A, Li D, Brueck SRJ (2004) Directed self-assembly of silica nanoparticles into nanometer-scale patterned surfaces using spin-coating. *Adv Mater* 16:1427–1432
- Xiong X, Hanein Y, Wang W et al (2001) Multi-batch micro-self-assembly via controlled capillary forces. In: Proceedings of RSJ/IEEE international conference on intelligent robots and systems. IEEE, Maui, HI, USA, pp 1335–1342
- Xiong X, Liang S-H, Bohringer KF (2004) Geometric binding site design for surface-tension driven self-assembly. In: Proceedings 2004 IEEE international conference on robotics and automation, Apr 26–May 1 2004. IEEE, New Orleans, LA, United States, pp 1141–1148
- Xu F, Finley TD, Turkyaydin M et al (2011a) The assembly of cell-encapsulating microscale hydrogels using acoustic waves. *Biomaterials* 32:7847–7855. doi:[10.1016/j.biomaterials.2011.07.010](https://doi.org/10.1016/j.biomaterials.2011.07.010)
- Xu F, Wu C-AM, Rengarajan V et al (2011b) Three-dimensional magnetic assembly of microscale hydrogels. *Adv Mater (Deerfield Beach, FL)* 23:4254–4260. doi:[10.1002/adma.201101962](https://doi.org/10.1002/adma.201101962)
- Xu L, Karunakaran RG, Guo J, Yang S (2012) Transparent, superhydrophobic surfaces from one-step spin coating of hydrophobic nanoparticles. *ACS Appl Mater Interfaces* 4:1118–1125. doi:[10.1021/am201750h](https://doi.org/10.1021/am201750h)
- Yamazaki A, Sendoh M, Ishiyama K et al (2004) Wireless micro swimming machine with magnetic thin film. *J Magn Magn Mater* 272–276:E1741–E1742. doi:[10.1016/j.jmmm.2003.12.337](https://doi.org/10.1016/j.jmmm.2003.12.337)
- Yang Y, Liu J, Zhou Y-X (2008) A convective cooling enabled freeze tweezer for manipulating micro-scale objects. *J Micromech Microeng* 18:95008
- Yeh H-JJ, Smith JS (1994a) Fluidic self-assembly for the integration of GaAs light-emitting diodes on Si substrates. *IEEE Photonics Technol Lett* 6:706–708. doi:[10.1109/68.300169](https://doi.org/10.1109/68.300169)
- Yeh HJ, Smith JS (1994b) Fluidic self-assembly of microstructures and its application to the integration of GaAs on Si. In: Proceedings IEEE micro electro mechanical systems an investigation of micro structures, sensors, actuators, machines and robotic systems, pp 279–284. doi:[10.1109/SENSOR.1994.555822](https://doi.org/10.1109/SENSOR.1994.555822)
- Yesin KB, Vollmers K, Nelson BJ (2006) Modeling and control of untethered biomicrobots in a fluidic environment using electromagnetic fields. *Int J Robot Res* 25:527–536. doi:[10.1177/0278364906065389](https://doi.org/10.1177/0278364906065389)
- Yeung BHB, Mills JK (2004) Design of a six DOF reconfigurable gripper for flexible fixtureless assembly. *IEEE Trans Syst Man Cybern Part C (Appl Rev)* 34:226–235. doi:[10.1109/TSMCC.2003.819704](https://doi.org/10.1109/TSMCC.2003.819704)
- Yim M, Shen W-M, Salemi B et al (2007) Modular self-reconfigurable robot systems [Grand challenges of robotics]. *IEEE Robot Autom Mag* 14:43–52. doi:[10.1109/MRA.2007.339623](https://doi.org/10.1109/MRA.2007.339623)
- Yin Y, Lu Y, Gates B, Xia Y (2001) Template-assisted self-assembly: a practical route to complex aggregates of monodispersed colloids with well-defined sizes, shapes, and structures. *J Am Chem Soc* 123:8718–8729

- Yin P, Yan H, Daniell XG et al (2004) A unidirectional DNA walker that moves autonomously along a track. *Angew Chem Int Ed Engl* 43:4906–4911. doi:[10.1002/anie.200460522](https://doi.org/10.1002/anie.200460522)
- Yuan Z, Petsev DN, Prevo BG et al (2007) Two-dimensional nanoparticle arrays derived from ferritin monolayers. *Langmuir ACS J Surf Colloids* 23:5498–5504
- Yurke B, Turberfield AJ, Mills AP et al (2000) A DNA-fuelled molecular machine made of DNA. *Nature* 406:605–608. doi:[10.1038/35020524](https://doi.org/10.1038/35020524)
- Zamanian B, Masaeli M, Nichol JW et al (2010) Interface-directed self-assembly of cell-laden microgels. *Small* 6:937–944. doi:[10.1002/sml.200902326](https://doi.org/10.1002/sml.200902326)
- Zenin VV, Novokreshchenova EP, Khishko OV (2011) Flip-chip bump-lead fabrication: a review. *Russ Microelectron* 37:107–113. doi:[10.1134/S1063739708020042](https://doi.org/10.1134/S1063739708020042)
- Zhe AAA, Jagtiani A, Vasudev A, Hu J, Zhe J (2011) Soft microgripping using ionic liquids for high temperature and vacuum applications. *J Micromech Microeng* 21:125025
- Zheng W, Jacobs HO (2004) Shape-and-solder-directed self-assembly to package semiconductor device segments. *Appl Phys Lett* 85:3635
- Zheng W, Jacobs HO (2006) Self-assembly process to integrate and connect semiconductor dies on surfaces with single-angular orientation and contact-pad registration. *Adv Mater* 18:1387
- Zheng W, Buhlmann P, Jacobs HO (2004) Sequential shape-and-solder-directed self-assembly of functional microsystems. *Proc Nat Acad Sci USA* 101:12814–12817
- Zheng W, Chung J, Jacobs HO (2006) Fluidic heterogeneous microsystems assembly and packaging. *J Microelectromech Syst* 15:864–870. doi:[10.1109/JMEMS.2006.878885](https://doi.org/10.1109/JMEMS.2006.878885)
- Zhu G, Nguyen N-T (2010) Particle sorting in microfluidic systems. *Micro Nanosyst* 2:202–216
- Zubir MNM, Shirinzadeh B, Tian Y (2009) Development of a novel flexure-based microgripper for high precision micro-object manipulation. *Sens Actuators A* 150:257–266. doi:[10.1016/j.sna.2009.01.016](https://doi.org/10.1016/j.sna.2009.01.016)